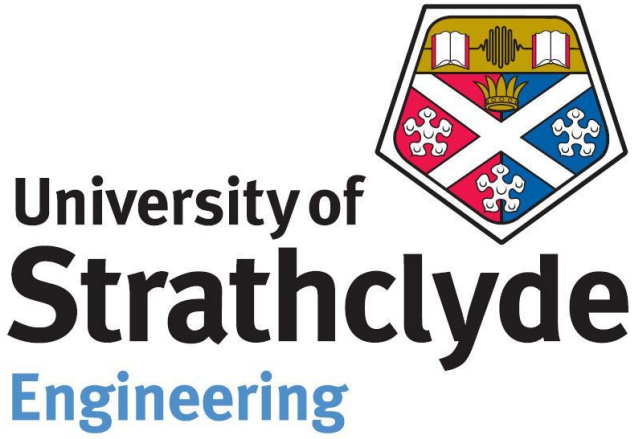

Whole body modelling of musculoskeletal interactions during whole body vibration to inform rehabilitation intervention design

Lewis Formstone

The Department of Biomedical Engineering

University of Strathclyde

A thesis presented in partial fulfilment of the requirements for the degree of MSc.

Supervisor: Dr. Sylvie Coupaud

August 2015

Declaration of Authenticity and Author's Rights

This thesis is the result of the author's original research. It has been composed by the author and has not been previously submitted for examination which has led to the award of a degree.

Signed: Date:

Acknowledgements

I would like to give special thanks to Dr Coupaud who not only lent her expertise to this project but also went above and beyond in providing both time and effort. I would also like to thank AnyBody Technology Inc. for providing me a trial licence to work on my project and the AnyBody community for their support.

Abstract

Background: A major secondary complication which can arise in individuals with spinal cord injury (SCI) is disuse-related bone loss as a result of long-term paralysis and immobilisation. An emerging rehabilitation technique used to treat this musculoskeletal degeneration is whole body vibration (WBV). This can be applied to patients in different body positions on a WBV platform in order to stimulate different muscle groups and in turn apply muscle forces to target bones. To treat the disuse-related bone loss, the hypothesis is that WBV intervention can stimulate bone formation indirectly via targeted muscle action, and/or directly if vibration acts as a mechanostimulus on the bone.

Aim & Objectives: The aim of this study was to develop whole body computational models of WBV intervention, to inform the design of intervention protocols in SCI patients. Effects of muscle loss were simulated, and activation and forces of different muscles analysed for a number of proposed configurations on the WBV platform.

Methods: WBV intervention was simulated using the AnyBody Technology Modelling software by implementing and adapting the currently available standing model. Different body positions (standing, knee flexed standing, squatting) and parameters of WBV such as frequency and amplitude were modelled and analysed, and the muscle actions simulated.

Results: Realistic muscle activities compared to the literature were found in all body position configurations without the WBV simulation. When modelling the WBV intervention, only the squatting body position and side-alternating WBV plate were found to give accurate results. The activities of several muscles were recorded in this configuration under a variety of frequencies and amplitudes. Finally muscle forces were analysed with changes in frequency and amplitude and found to cause a corresponding change in the loading of regions the bones of the ilium, tibia, femur, ischium, fibula, sacrum and coccyx. The aim is for the results of this model to be used in the future to inform WBV protocol development for musculoskeletal rehabilitation in SCI and other target patient groups.

List of Figures

Nomenclature

a	Acceleration (mm/s^2)
AMMR	AnyBody managed model repository
ANS	Autonomic nervous system
AP	Action potential
BF	Biceps femoris
BMD	Bone mineral density
C	Coefficient-matrix for the unknown forces of the AnyBody optimisation problem
d	All known applied loads and inertial forces of the AnyBody optimisation problem
DoF	Degree of Freedom
d_{p-p}	Peak-to-peak displacement in the y-axis (mm)
EMG	Electromyogram
EMGrms	Root mean square of the EMG signal
f	Unknown forces of the AnyBody optimisation problem
FES	Functional electrical stimulation
$f^{(M)}$	Muscle forces of the AnyBody optimisation problem
$f^{(R)}$	Joint reaction forces of the AnyBody optimisation problem
f_{vib}	Vibration frequency (Hz)
g	Gravity (approx. $9.81\ m/s^2$)
G	Objective function of the AnyBody optimisation problem
GM	Gluteus maximus
GN	Gastrocnemius
LIUS	Low-intensity ultrasound
LIV	Low-intensity vibration
MVC	Max voluntary contraction
N_i	Normalising factor (muscle strength) of the AnyBody optimisation problem
$n^{(M)}$	Integer number of bodies in the system of the AnyBody optimisation

	problem
R_{fat}	Mass fraction of fat in the AnyBody AUUHuman body model
R_{muscle}	Mass fraction of muscle in the AnyBody AUUHuman body model
R_{other}	Mass fraction of other body composition variables in the AnyBody AUUHuman body model
RF	Rectus femoris
RMS	Root mean square
SCI	Spinal cord injury
sEMG	Surface electromyogram
SNS	Somatic nervous system
VL	Vastus lateralis
WBV	Whole body vibration

Contents Page

Chapter 1: Background

1.1 Aims and Objectives

A deleterious condition faced by the majority of individuals with spinal cord injury (SCI) is the rapid bone loss which occurs after injury known as osteoporosis. One of the reasons for this bone loss is thought to be due to the intrinsic relationship between mechanical loading of the bone and bone remodelling, which is disturbed during SCI induced immobilisation. A recently developed method which has shown to be successful in treating other pathologies involving disuse related osteoporosis is whole body vibration (WBV). One way this therapy compensates for the lack of mechanical loading on the bone is by stimulating the muscles which causes indirect loading of the bones via muscle forces. WBV has been shown to be effective at preventing bone loss in a case study of an individual with a SCI performed by Davis et al (1) but otherwise research into the effects of WBV on SCI related osteoporosis is limited. This is problematic considering the effects of WBV on the skeleton are still not fully understood and therefore the correct WBV parameters, such as frequency and amplitude of vibration, to best treat bone loss in individuals with SCI are not yet known. One way the effect of different parameters of WBV on muscle behaviour has been studied, without requiring numerous clinical trials to investigate each parameter, is the use of AnyBody computational models. This has been used in the past by Ma et al (2) as a method of determining the muscle activities of healthy individuals in different body positions during WBV.

The aim of this study is to widen the parameters of WBV tested by Ma et al to include the effects of different frequencies, amplitudes, and platform type of WBV on muscle action. In addition the individual will be modelled to replicate the effects of a SCI rather than a healthy individual to enable the model to inform this field. Finally, since the muscle forces are involved in loading of the bones, the approximate location and magnitude of the loading on the bones by a few selected muscles will be identified.

The overall aim of this report is to gain a better understanding of how the bone loading via muscle forces in an individual with SCI changes under a range of WBV parameters. It is hoped that this information will make it possible to tailor the treatment of WBV to target specific bones by activating specific muscles. To summarise, this simulation will provide information of which WBV parameters to choose in order to maximise the forces on certain bones of an individual with SCI induced osteoporosis.

1.2 Functional anatomy of the lower limbs

1.2.1 Skeleton

The skeleton of the lower limbs is split into the girdle and the skeleton of the free limbs. The girdle, also known as the pelvic girdle, is subsequently split into the two coxal bones. Each coxal bone is made up of three smaller bones fused together, the ilium, ischium and pubic bone. The pelvic girdle is responsible for transmitting the weight of the vertebral column down to the lower limbs. Each of the hip bones bears a cup-shaped socket called the acetabulum which connects to the lower limbs by receiving the head of the femur, the bone of the thigh. The pelvis is connected to the spine by the hip bones which meet the inferior end of the vertebral column, the sacrum and coccyx (3).

Further down the body at the lower leg are the tibia and fibula. The tibia is the larger of the two bones which articulates at the knee and ankle and is responsible for transmitting most of the weight. The fibula is the site of many muscle attachments and enters into the articulation at the ankle but not the knee. The knee joint between the femur and tibia, and the ankle joint can both be considered largely to be hinge joints (3).

Located below the ankle joint are the seven tarsals arranged to transmit weight to the heel and the ball of the foot. Movement between these bones allows much of the foot's inversion and eversion capabilities. These bones connect to the metatarsals which form much of the instep of the foot. Lastly, the metatarsals articulate with the proximal phalanges of the digits. A diagram of the lower limbs skeleton is shown in Figure 1.

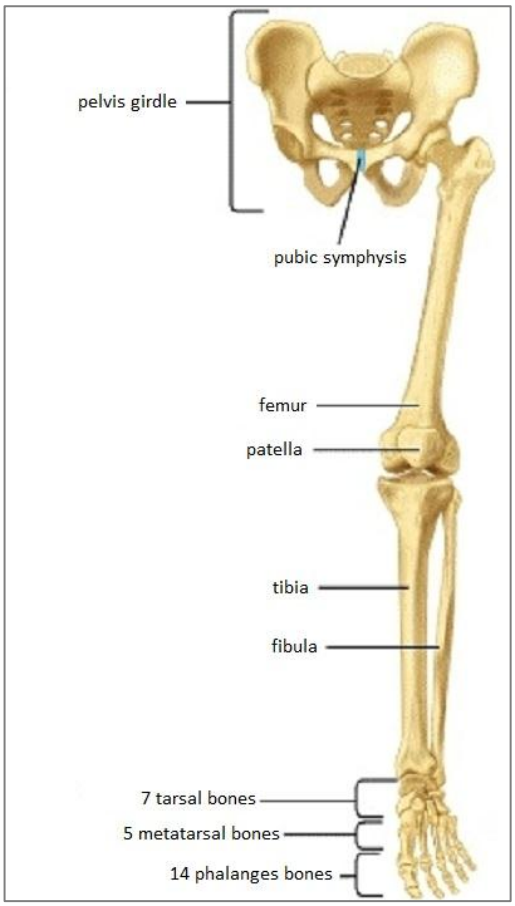

Figure 1: Bones of the lower limbs, taken from (4)

1.2.2 Muscles

The muscles which act on the lower limb can be arranged into three groups. These are the muscles which move the thigh, those that move the lower leg, and those which move the ankle, foot, and toes. The skeletal muscles described in this section are attached to the body at two points called the origin and insertion. The origin point of the muscle is located at a bone which is relatively stable during the contraction, while the insertion point may be located at bone, tendon, or connective tissue, which has greater motion during the contraction (3).

The muscles responsible for moving the thigh are large powerful muscles and can be grouped into the gluteal group which make up the buttocks, the lateral rotator group, adductor group, and the iliopsoas group. The muscles which move the leg are split into those which flex the knee including the biceps femoris and semimembranosus and those which extend the knee including the rectus femoris and vastus intermedius.

Lastly the muscles of the foot and toes can be split into muscles which dorsi flex or plantar flex the ankle and the digital flexors and extensors at the toes.

A study by Loram et al (5) has identified the muscles most active in the standing position to be the soleus and gastrocnemius. These muscles are located in the lower leg and act to plantar flex the ankle. The body centre of mass is located in front of the ankle joints during standing and these muscles are required to stop the body from toppling forwards as a result.

The squat position varies according to individual preference and as a result there is some discrepancy in the muscle activities recorded according to the study performed. One study by Isear et al (6) investigated the lower extremity recruitment patterns during several motions of unloaded squats using sEMG. The results of this study showed that the dominant muscle group involved was the quadriceps, although significant activity was also measured in the hamstrings, gastrocnemius, and gluteus maximus.

1.3 Bone

1.3.1 Bone remodelling

Bone remodelling is an active and dynamic process which depends on a correct balance between the action of bone resorption, performed by osteoclasts, and bone deposition, performed by osteoblasts (7). In order for a healthy bone mass to be maintained it is crucial that there is a well regulated coupling between these two processes quantitatively, as well as in time and space. The ability of bone to act as a dynamic tissue which can renew during the life of an individual is a crucial process. This is important for a number of applications such as allowing the substitution of infantile bone with secondary bone, which is more mechanically competent; or repairing bone which has developed micro-fractures (7). There are however cases where the dynamic behaviour of bone causes deleterious effects. This can be seen in conditions which cause perturbation in the regulation of bone formation and resorption. The result of this can be an accelerated bone gain as seen in osteopetrotic states or accelerated bone loss as seen in osteoporosis (8).

1.3.2 Osteoporosis

This condition is characterised by a reduction in bone mass and a deterioration of the skeletal microarchitecture in the affected areas (9) which in turn leads to increased bone fragility and an increase in fracture risk (10). Based on this definition it is apparent that the reduced bone mineral density (BMD) is a major determinant in the increased fracture risk. Since it is possible to make accurate and precise measurements of bone mineral content or density, this measurement is used to form the operational definition of osteoporosis in studies (11).

The onset of osteoporosis has been divided into two categories. The first type includes conditions which are not caused by some specific disorder, known as primary osteoporosis. The second type includes bone loss which is caused by specific diseases or medications and is known as secondary osteoporosis (12).

Primary osteoporosis is the most common form of the disease. The majority of sufferers are the elderly with an onset occurring as the result of the cumulative impact of bone loss and the deterioration of bone structure which occurs as people age. Other sufferers are postmenopausal women who have an increased risk of suffering from the condition due to a reduced production of oestrogen after menopause, a key hormone in bone growth in females (13). A rarer case of osteoporosis is found among younger individuals, and is often referred to as “idiopathic” osteoporosis since in many cases the exact causes of the disease are unknown (12).

Individuals who suffer from secondary osteoporosis normally experience greater levels of bone loss than would be expected for a normal individual of the same age, sex, and race. There are several genetic diseases which have been linked to secondary osteoporosis, the most common of which are idiopathic hypercalciuria and cystic fibrosis. Other conditions associated with osteoporosis include endocrine disorders and gastrointestinal diseases. Finally, there are other sources of osteoporosis which are not easily categorised. An example of this is osteoporosis which is caused in part or fully as a result of immobilisation as experienced by bed rest patents or individuals with SCI (12), known as disuse osteoporosis.

1.4 Spinal cord injury

1.4.1 Incidence

SCI is a serious and life-long medical condition often leading to permanent disability of the affected individual (14). There are two ways damage may be incurred to the spinal cord, either by traumatic or non-traumatic means. Traumatic SCI results from trauma by a variety of causes including falls or car accidents. Non-traumatic SCI, on the other hand, is normally the result of some underlying pathology such as infectious disease, tumour or a congenital disease such as spina bifida.

Obtaining accurate figures for the incidence of SCI is difficult due to factors such as difficulty in classifying the injury (15). Figures which are available estimate there are currently 50,000 people living in the UK with SCI with another 1000 people sustaining SCIs per year (16).

There is recent evidence which indicates that the age demographic of those who suffer from SCIs is shifting. Historically in developed countries SCIs have mainly been sustained by younger people aged between 21 and 30. In recent years however there is evidence of increasing incidents among older people (17). This is shown by a study by Thompson et al (18) at a SCI unit in Quebec which found that there was a 13-year average increase in age of individuals who suffered traumatic SCIs between the years 2002 and 2010.

1.4.2 The medical condition

The spinal cord is made up of bundles of nerves which are responsible for the transfer of motor and sensory information between the brain and body. The spinal cord is contained with the spinal column which is divided into several regions. These are made up of three mobile regions, the cervical spine, thoracic spine, and lumbar spine; and two fused regions, the sacrum and the coccyx (19). These regions and the corresponding nerves of the spinal cord are shown in Figure 2.

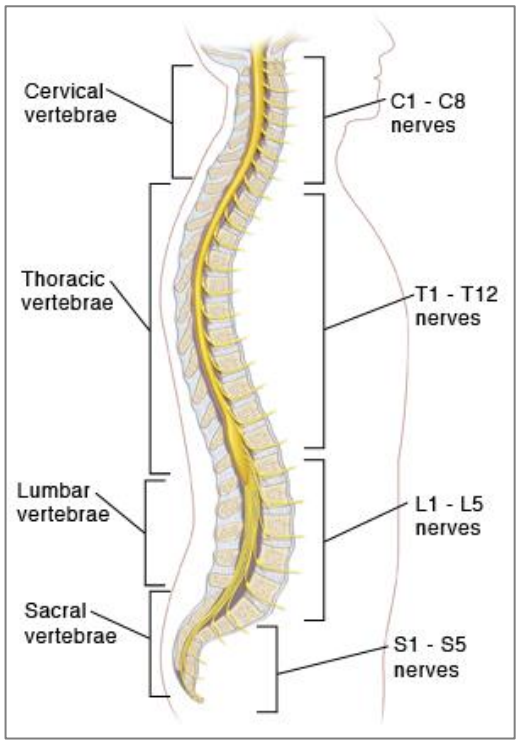

Figure 2: Diagram of the Spinal Cord, taken from (20)

The whole of the human nervous system is made up of the brain, spinal cord, sensory organs, and the other nerves which are required to connect these organs to the rest of the body. Functionally it can be split into the somatic nervous system (SNS) responsible for voluntary skeletal muscle control and the autonomic nervous system (ANS) responsible for unconscious control such as breathing and digestion. The autonomic nervous system can be further divided into the sympathetic ANS and parasympathetic ANS which work together to maintain body homeostasis. The sympathetic ANS primary role is to stimulate the body's flight-or-fight response while the parasympathetic ANS is responsible for stimulating the "rest-and-digest" activities of the body including digestion, urination, and salivation (3).

Depending on the level of trauma to the spinal cord nerves these systems may be damaged interrupting the transmission of signals to the rest of the body. A SCI is classified as a lesion to the spinal cord which results in a change in the conduction of sensory and motor signals in the nerves across the lesion. Different levels of the spinal cord correspond to areas where certain nerves enter and exit the body to certain parts of the body. As a consequence, the different levels are associated with

certain losses of motor and autonomic function which typically occurs below the level of impact to the spinal cord.

1.4.3 Classification of injury

The determination of injury severity is achieved via an examination according to the International Standards for Neurological Classification of SCI (21). The most important determinant of long term prognosis is whether an injury is clinically complete or incomplete (22). A complete SCI is defined as the complete absence of sensory and motor function in the lowest sacral segments (S4-S5) whereas an incomplete injury retains partial preservation of sensory and/or motor function in this region.

In addition to the completeness of the injury, there are broad groups used to describe the level of impairment of the individual. The term tetraplegia refers to the impairment or loss of motor and/or sensory function in the cervical segments (C1-C8) of the spinal cord leading to an impairment of the arms as well as typically the trunk, legs and pelvic organs. The term paraplegia refers to the impairment of motor and/or sensory function in any of the regions below the cervical segments (T1-S5) of the spinal cord leading to retention of arm function but possible impairment of the trunk, legs and pelvic organs depending on the exact level of injury (21).

Finally, the term chronic SCI is used to refer to a level of paralysis which lasts for a long duration, usually defined as more than one year post injury.

1.4.4 Secondary complications

1.4.4.1 Common complications

Individuals with SCI can suffer from a range of secondary medical complications which are important considerations in long term care and quality of life. A study by McKinley et al (23) used data from the SCI Statistical Centre, located in the USA, which examined the long-term complications suffered by individuals after traumatic SCI. This study found that the most frequent secondary medical complications suffered by individuals with SCI were pressure ulcers caused by prolonged pressure to the skin. Another common condition identified was autonomic dysreflexia which

occurs in individuals with a neurologic level of SCI at or above the sixth thoracic vertebral level (T6). This condition is normally triggered by a painful stimulus below the level of the SCI. The stimulus causes intact lower motor neurons to transmit the message up the spinal cord. When the information reaches the location of major sympathetic ANS outflow (T5-T6) a sympathetic response is stimulated causing vasoconstriction and leading to hypertension. The site of the SCI creates a disconnect in the feedback of the ANS meaning the parasympathetic branch is not able to counteract the effects of the sympathetic ANS (24). The third most common complication identified was due to pneumonia and atelectasis. This condition is a risk to individuals with a SCI at the cervical or high thoracic level and is caused by a paralysis of the respiratory muscles below the level injury, resulting in a weak cough mechanism and difficulty in mobilising lung secretions (25).

1.4.4.2 Musculoskeletal degeneration

In addition to the aforementioned complications, individuals with SCI have also been observed to suffer from musculoskeletal degeneration involving a loss of muscle (26) and bone mass. These conditions result in further complications for the affected individual.

The effects of muscle atrophy have been reported to cause decreased metabolic rate and increased fat storage in individuals with SCI (27). The scale of the reduction of muscle mass has been quantified in a study by Wilmet et al (28) which used dual-energy X-ray absorptiometry to determine that the lean muscle mass of 31 patients with complete SCI. This study found a reduction of muscle mass of approximately 15% after 1 year, with a rapid reduction occurring 15 weeks after injury. Confirmation of this result is provided by a study by Modlesky et al (29) which measured the same percentage muscle loss using X-ray absorptiometry and magnetic resonance imaging of 8 individuals, also with complete SCI.

Another secondary complication of SCI and the focus of the intervention in this project are long bone fractures caused by osteoporosis. Osteoporosis is a condition which is known to occur in a majority of patients with SCI (9) with an onset of bone loss as early as 6 weeks post injury (30). Complications from fractures suffered by

individuals with SCI as a result of osteoporosis are known to lead to increased morbidity, decreased functional mobility, and increased attendant care (31).

The patterns of bone loss seen in osteoporosis from etiologies such as endocrine diseases or nutritional disorders differ from those observed in disuse related SCI. A reduction in BMD and bone mineral content has been documented in the pelvis and lower extremities in persons with paraplegia whereas persons with tetraplegia also suffer from bone loss in the upper extremities. The most severe bone demineralisation is understood to occur in the lower limbs (9). This has been demonstrated by Dauty et al (32) in a study of 31 SCI patients 1 year after injury which showed a reduction in bone mass of 52% and 70% at the distal femur and proximal tibia respectively.

The exact mechanisms of bone loss in SCI are not fully understood although there are a number of factors which are thought to contribute. One factor is a reduction in the mechanical loading on the bone (33) as explained in more detail later in the report. Another contributing factor is a lesion induced increase in the intra-medullary pressure measured in individuals with SCI (34). This has been found to cause delayed blood flow which in turn disturbs bone formation by effecting bone cell differentiation. A final factor is the measured reduction in growth factors (35). These growth factors are known to play a major role in bone metabolism and thus it is thought that a reduction could be involved in bone resorption. The overall imbalance in bone formation and resorption following SCI is thought to be the result of increased osteoclast activity over osteoblast activity (36).

Chapter 2: Literature Review

2.1 Current treatments for bone loss in SCI

2.1.1 Pharmacologic treatment

A rapid increase in urinary calcium has been observed in individuals immediately after SCI (37) resulting in a negative calcium balance. This phenomenon has also been observed in individuals undergoing long term bed rest and attempts to treat it have been performed by supplementing the individual with calcium and vitamin D. The effect of this has been to achieve a calcium homeostasis but fail to prevent the occurrence of disuse osteoporosis in bed rest subjects (38). Similarly phosphate supplements have been shown to increase the calcium balance of best rest patients but bone loss still occurred (39).

Another treatment tested is the use of calcitonin. Calcitonin is a potent inhibitor of bone resorption which works to inhibit the action of osteoclasts by reducing their mobility, number, and secretion activity (40). Calcitonin has been demonstrated to be successful in reducing bone loss long term in postmenopausal women (41) but has been found to be ineffective as a treatment for osteoporosis in paraplegic rats (42).

Biphosphonates are a well-established class of drugs used in the treatment of osteoporosis. Biphosphonates have a high affinity for bone but not for other tissues. By binding to the bone mineral they confer an antiresorptive property which inhibits bone resorption. A recently developed bisphosphonate, alendronate has been demonstrated to have a positive effect on BMD in a study of 19 chronic SCI patients of varying completeness of injuries by Moran de Brito et al (43). This study is however limited by a relatively small sample size and only found a statistically significant increase in 2 out of 12 densitometric parameters compared to the control. Further support for the effectiveness of this class of drugs is demonstrated by a study using intravenous pamidronate, an early-generation bisphosphonate, by Nance et al (44). In a nonrandomised control trial of 24 subjects with complete or motor-incomplete SCI within 6 months of their injury it was found that treated patients had

significantly less bone density loss compared to the control who did not receive pamidronate.

2.1.2 Non-pharmacologic treatments

There are a number of non-pharmacological treatments being used or investigated for the prevention of bone loss in individuals with SCI. The reduction of bone loading in SCI is thought to be a major factor in bone loss as observed in studies of prolonged bed-rest and weightlessness (45). Therapies implemented include the use of standing or orthotically aided walking (32) and physical exercise (46). These therapies attempt to counter the lack of weight-bearing created by SCI by re-stimulating the bone segments to return as closely as possible to their pre-lesional physiological condition.

The effect of functional electrical stimulation (FES) has also been tested for its behaviour on the bone. Functional electrical stimulation uses electrical currents to activate nerves causing muscle contractions. These muscle contractions produce tension on the bone and in doing so may help to preserve bone mass. There has been some success shown in this therapy method in a study of 12 individuals with motor-sensory complete SCI by Frotzler et al (47). This study used FES induced high volume cycle training to reverse the bone loss substance in the legs with a significant increase in the BMD observed in the femur.

Another therapy tested is the application of low-intensity ultrasound (LIUS). The underlying mechanisms of this process on the bone are not yet fully understood although it is known that the increase in fracture healing it produces is due to induced mechanical strain imparted on cells (48). There has been evidence of the ability of LIUS to act as an osteogenic stimulus in a study of adult mice by Lim et al (49). In this study female rats were ovariectomized to replicate post menopause-related osteoporosis and the application of LIUS was found to be effective in preventing bone loss compared to a non-treated group. There is however no evidence that this effect can be replicated in SCI induced osteoporosis. This is exhibited by a study by Warden et al (50) which found the use of pulsed LIUS to be ineffective in preventing osteoporosis in a group of 15 individuals with incomplete and complete SCI.

Finally, one of the most recent therapies tested for bone mass preservation in SCI is WBV. This therapy uses a platform to apply vibration to a subject either in isolation of combined with exercise.

2.2 Whole body vibration

2.2.1 History

While the detrimental effects of vibration have long been understood, the beneficial effects of vibration are still being discovered today. One of the first human studies which explored the positive effects of vibration was performed by Sanders (51) and studied whether an oscillating bed could be used to counteract cardiovascular and musculoskeletal de-conditioning. Since this time there have been many advances in the field, driven by a greater understanding of the mechanisms of vibration on the body and improvements in technology. This has led to an increase in research into the potential of WBV as both a therapeutic intervention and an exercise modality. The subject of most interest in this review is the potential benefits of WBV as a treatment to bone loss undergone by individuals with SCI.

2.2.2 Operation of Whole Body Vibration

WBV can be considered as forced oscillation, where energy is transferred between the actuator (vibration device) to the resonator (the subject) (52). The vibration applied to the subject is most often of a sinusoidal shape and can therefore be fully described by its amplitude, frequency and phase angle as illustrated in Figure 3.

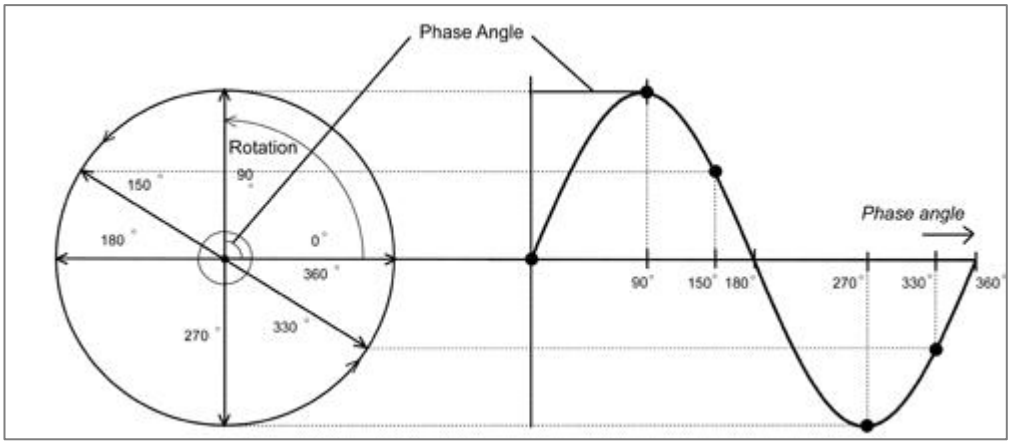

Figure 3: Sinusoidal waveform, taken from (53)

There are two main types of platforms which are used to transfer the energy to the subject. The first of these uses oscillatory side-alternating motion over a central fulcrum, lifting one side of the body while lowering the other alternatively, which delivers a different amplitude of vibration depending on the position of the feet. The second is a vertical vibration plate which drives the platform upwards and downwards and maintains equal amplitude across the plate (31). Both of these platforms are illustrated in Figure 4.

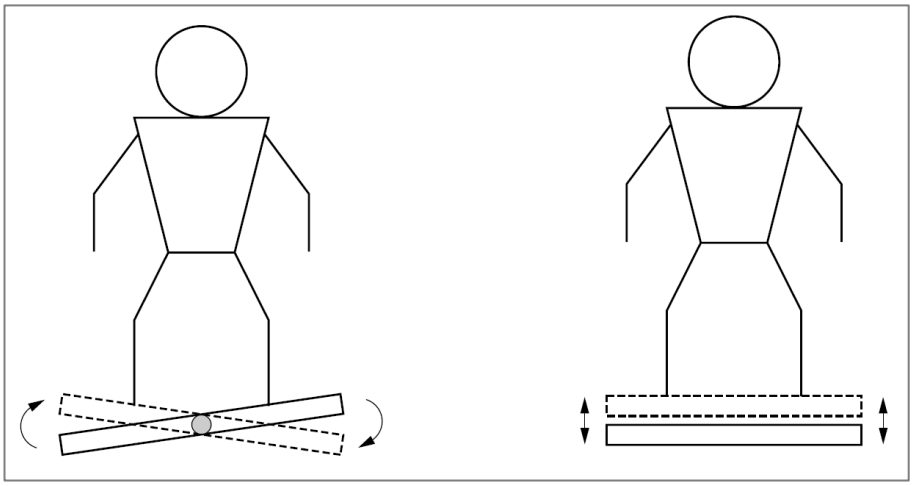

Figure 4: Side-alternating and vertical vibration platforms, taken from (54)

The amplitude of vibration can be quoted as the maximum displacement from equilibrium (in millimetres) known simply as the amplitude. Alternatively the amplitude may be described by the peak-to-peak displacement which measures the displacement between the lowest and highest points of the platform and is equal to twice the amplitude from equilibrium. The difference between amplitude from equilibrium (C – B) and peak-to-peak amplitude (C – A) measurements are shown in Figure 5.

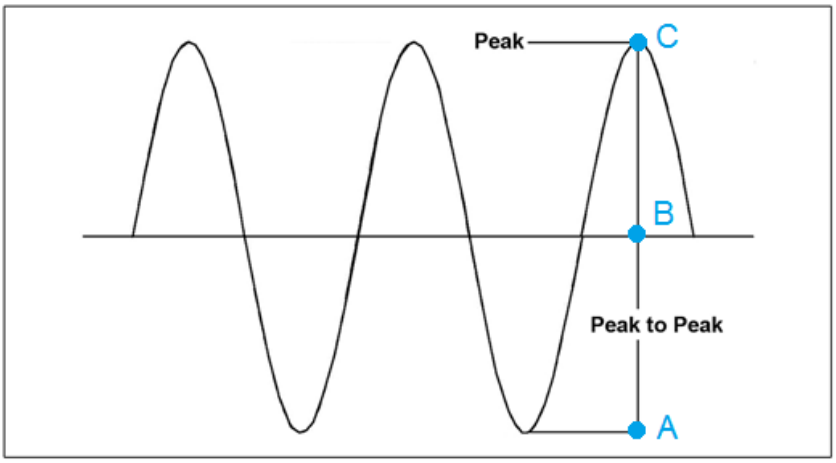

Figure 5: Amplitude from equilibrium vs. peak to peak amplitude, adapted from Totosy et al (31)

A commonly used descriptor of vibration is the peak acceleration applied to the subject. This can be calculated from the frequency and peak-to-peak displacement as shown in Equation 1. In order to facilitate comparisons between studies, the value of acceleration is normally presented in multiples of the earth's gravity (55).

$$a = 2 * \pi^2 * f_{vib}^2 * d_{p-p}$$

Equation 1: Acceleration produced by WBV, taken from Totosy et al (31)

Where a= acceleration (mm/s^2), f_{vib}= vibration frequency (Hz), d_{p-p}= peak-to-peak displacement in the y-axis (mm)

2.2.3 Methods of applying WBV in SCI patients

One of the technical difficulties present in delivering WBV to individuals with SCI is the acute paralysis of the individual which can cause difficulty in achieving an upright position. One way this has been overcome is by delivering WBV while the individual is in a supine position on a tilt table either with the knees straight (56) or flexed (57). Another method of delivering WBV to an individual with SCI has been by assistive standing using a standing frame, allowing the individual to stand erect (1) (58) or at a variety of knee flexion angles (59). Images of individuals in the tilt table and standing frame are shown in Figure 6 and Figure 7 respectively. A final method of supporting individuals with SCI undergoing WBV identified has been the use of upper body harness to unload the body weight (60). Finally in a study with

subjects with motor incomplete SCI, subjects were able to stand unaided on the platform with knees flexed at approximately 30° (61).

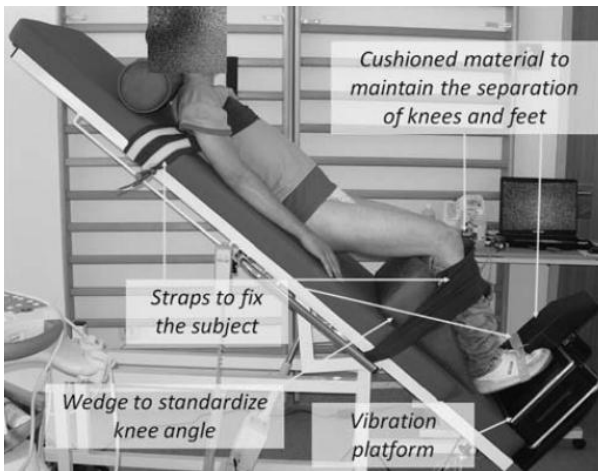

Figure 6: Placement of subject on the tilt table during the application of WBV, taken from Herrero et al (57)

Figure 7: Placement of subject in standing frame during application of WBV, taken from Davis et al (1)

2.2.4 Measuring muscle activity

The measurement of muscle activity has played an important role in a number of WBV studies such as to assess the response of individuals with SCI (57) and other fields including as a training modality for healthy adults (62). The typical method of experimental muscle activity measurements are performed using surface electromyogram (sEMG). The sEMG uses surface electrodes which are placed on the skin above the muscle which is to be measured.

The measurand is an electrical signal generated by the muscle. The muscle itself is made of numerous muscle fibres which lay parallel together with connective tissue. Forces are produced by muscle contractions stimulated by motor units of the muscle which consist of a number of muscle fibres innervated by a single motor neuron. When the central nervous system requires the contraction of a specific motor unit, there is a release of neurotransmitters which cause a charge change called an action potential (AP). This AP propagates down the motor neuron to the muscle fibres within the motor unit causing the contraction of all muscle fibres connected to the motor neuron. Since real muscle contractions require the contraction of many motor units, the resulting EMG recording is therefore a complex summation of many motor unit APs (63).

The measured EMG signal is comprised of both a positive and negative signal which means the mean amplitude of each EMG signal is approximately zero, regardless of the activation level of the muscle. In order to get a realistic mean value the signal must be rectified or squared prior to analysing. The most common way this is performed is by calculating the root mean square (RMS) of the signal, the EMGrms. This is a calculation of the square root of the average value of the square of the signal (64).

2.2.5 Physiological effect upon bone

Wolff's law states that bone mass adapts to the mechanical loading applied as well as metabolic influences (65). The effect of mechanical loading on the bone is due to a behaviour called mechanotransduction whereby the bone cells respond to a variety of mechanical signals, including strain magnitude and strain frequency. The idea that bone loading is essential for maintaining healthy bone mass has been described by the Daily Stress Stimulus Theory. This theory proposes that there is a threshold daily stress required by the bone and any daily stress stimulus below or above this value will result in net bone loss or gain respectively.

One way in which WBV is thought to activate mechanotransduction in the bone and stimulate osteogenesis is by direct loading of the skeleton. This effect has been studied by Hsieh et al (66) in rats by exposing them to dynamic loading frequencies of between 1 and 10 Hz to produce perturbations of the intramedullary pressure. This change in pressure resulted in fluid flow which consequently caused shearing stresses on the cell membranes. The conclusions of the study were that cellular deformation caused by shear stress was linked to an activation of osteogenesis and consequently bone remodelling. There have been a number of explanations as to why extracellular fluid forces have such a cellular response including activation of membrane mechanoreceptors, focal adhesion proteins, or cytoskeletal signalling (31).

The other action of WBV in bone remodelling is by forces produced by muscle contraction on the skeleton. The theory that muscle loading has an effect on bone growth is supported by Harold Frost's mechanostat hypothesis (67). In short this theory states that it is the muscles forces which create the peak forces acting on the bone and thus muscle and bone growth and adaptation are intrinsically linked.

Muscle contractions during WBV are thought to be activated by monosynaptic and polysynaptic neural pathways which generate a "tonic vibration reflex" (31). The tonic vibration reflex has been observed to cause the muscle to contract and relax continually over the course of the stimulus (68) indicating the suitability of WBV in achieving bone loading in this way. The intrinsic relationship between muscle strength and bone loss has been validated by the work of Zhou et al (69) which found a significant relationship between a reduction in muscle strength and a reciprocal decline in BMD in postmenopausal women.

2.2.6 Effect of WBV parameters on bone characteristics

Up until this stage only the ways in which WBV imparts a load on the bone has been discussed. In reality, the success or failure of WBV in influencing the bone remodelling of a given individual is dependent on a far greater number of variables.

2.2.6.1 Type of loading

The two ways in which WBV acts to load the skeleton have already been discussed but just as important is the type of loading which is transmitted to the bone. This has been outlined by Turner (70) who published a paper of the three fundamental rules which govern bone adaptation. The first of these is that the loading should be dynamic rather than static which is already the case in WBV. The second rule is that bone adaptation requires only a relatively short duration of loading. This is optimal for WBV as it means that theoretically short sessions of WBV will be as effective as longer ones. This has been validated by the work of Rubin and Lanyon (71) in animal studies which found that a few loading cycles of vibration of relatively high magnitudes were just as effective at stimulating bone formation as those when the loading cycles were increased 10-fold. The final rule is that bone cells become accustomed to routine mechanical loading. This can be overcome using WBV by positioning the patient in different body positions and performing certain exercises during loading.

2.2.6.2 Platform type

The influence of platform type on neuromuscular activity has been demonstrated by Ritzmann et al (72) . This study found that side-alternating vibration resulted in

significantly greater EMG activity than vertical vibration at all conditions tested. This has significance when considering the role muscle contractions have on bone formation. An explanation for this result has been provided by Pel et al (73) whose research found that side-alternating vibration generated acceleration magnitudes twice as high as vertical vibration in the lower limbs, and thus generated greater muscle activity, due to a smaller damping effect at the ankle.

Evidence looking at the direct biological effects the platform type has on bone characteristics is sparse. There is however one study which has linked the side-alternating platform to a greater production of procollagen type 1 N-propeptide, a biomarker in bone formation (74) compared to the vertical vibration platform.

2.2.6.3 Body position

An important factor when targeting certain bones with WBV is the transmissibility of vibration. A major factor of transmissibility has been found to be the knee joint angle of the subject when WBV is administered. The effect of joint angle on transmissibility has been studied by Rubin et al (75) under side-alternating low magnitude vibration (<1 g) and a frequency of 25 Hz. This study found that the transmissibility at the hip and spine was approximately 80% when standing erect, but decreased to 60% in a relaxed stance, and down to 30% when the subject had a 20 degree knee flexion.

In studies where muscle forces are utilised in the therapy for bone loss, the muscle activation due to body position is considered to be important. A study by Ritzmann et al (72) studied the effects of knee flexion of 18 healthy subjects found that increasing knee flexion angles (5-60°) resulted in a significant increase in EMG activity of knee extensor muscles and a significant reduction in ankle plantar flexor muscles.

2.2.6.4 Magnitude

The effect of the magnitude of vibration on bone characteristics appears to be very dependent on the patient group tested. Experiments utilising magnitudes of less than 1 g have shown success in animal studies as demonstrated in a study by Pasqualini et al (76). This study found that the application of vertical vibration at a frequency of 90 Hz on mature rats resulted in beneficial effects in the long bones and vertebra.

Similarly magnitudes as low at 0.3 g have shown to be effective to increase bone density in female children with low bone density (77).

On the other hand magnitudes of below 1 g have not been shown to have a similar effect amongst older adults. This is illustrated by a study by Rubin et al (78) on postmenopausal women which used vertical WBV at magnitudes of 0.2g in a trial of 70 post-menopausal women but found no significant changes in bone density. Higher magnitudes of vibration have however shown positive effects on the bone density of older adults. This is evidenced by a study by Verschueren et al (79) of 70 post-menopausal women aged 58-74 years old which found that vertical WBV of amplitude 2.28-5.09 g caused a significant increase in the BMD of the hip.

A final observation from the literature is that WBV appears not to have any effect on the bone density of individuals who are young and already have healthy levels of bone density. This is shown by a study by Torvinen et al (80) in a study of 56 volunteers aged 19-38 years old. This study found no changes in bone characteristics over 8 months of vertical WBV at magnitudes of 2-8 g. The reason offered for this by the author is that since the participants were young and healthy their bones had no physiological need to adapt to any kind of loading and so remained unchanged.

2.2.6.5 Frequency

Typically investigations and interventions involving WBV therapy or training take place at 15-35 Hz in order to achieve maximum transmissibility of the mechanical stimulus provided by the plate (75), and to avoid resonant frequencies. Resonant frequencies can pose a major problem in vibration studies and occur when an object is forced to vibrate at its natural frequency, resulting in oscillation at the object's maximum amplitude and acceleration.

Beneficial effects on bone have been shown using both high and low frequency vibrations on postmenopausal individuals. An example of a study of bone loss which utilised relatively high frequencies has been performed by Verschueren et al (79). This study used a vertical vibration plate with frequencies of between 35 and 40 Hz to increase BMD of the hip in a group of 70 postmenopausal women. An example of a study which utilised low frequencies to achieve a similar effect is a study by Gusi

et al (81) on 28 postmenopausal women. In this case side-alternating WBV at a frequency of 12.6 Hz and 3 mm amplitude was used to achieve a significant increase in BMD at the femur compared to a walking only group.

2.2.7 Effect of vibration on bone loss by subject populations

2.2.7.1 Older adults and post-menopausal women

Osteoporosis is one of the most common metabolic diseases and a leading cause of morbidity and mortality in the elderly population, especially amongst postmenopausal women (82). Both aging and the postmenopausal period have been linked to changes in the BMD in elderly subjects. The results of WBV to treat this reduction in BMD have been mixed. A study of eight months of vertical WBV (20 Hz, 2 mm) training on a group of 37 elderly women was found to produce no beneficial effects on the bone (83). Similarly a study of side-alternating WBV over 12 months (20 Hz, 3-4 mm) on 22 postmenopausal women yielded inconclusive results in improving bone quality (84). A successful 6 month study (35-40 Hz, 1.7-2.5 mm) used vertical WBV in combination with static and dynamic knee-extensor exercises and significantly increased the BMD of the hip (+0.93%, $P<0.05$). Another successful study utilised side-alternating vibration at lower frequencies and amplitudes (12.6 Hz, 3 mm) on a group of 28 post-menopausal women (81) and yielded an increase in the BMD of the femur of the WBV group of 4.3% ($P=0.011$) compared to a walking group.

2.2.7.2 Astronauts and bed rest

The space race of the 1960's led to extensive research into the therapeutic effects of vibration for the first time. This was a consequence of the US and Russian space programmes identifying and examining methods to treat the effects of zero gravity conditions on the deterioration of BMD and muscle tissue (85). An early study by Goodship et al illustrated the effectiveness of localised vibration over long term (5 month) space flight. The results showed no reduction in BMD of the mechanically stimulated heel bone compared to a 7% decline in the BMD of the non-stimulated heel bone (86). A further study has tested heathy subjects undergoing extended bed rest as a ground-based analogue for spaceflight (87). This study found that the

application of short intervals of low magnitude (0.3 g) vibration was effective at preventing bone loss due to non-weight bearing.

2.2.7.3 Spinal cord injury

Individuals with SCI suffer from rapid bone loss due in part to a reduction in muscle activity and mechanical loading. The result of this is increased risk of low-trauma fracture (26). Currently there are a limited number of studies available into the effect of WBV on the bone health in SCI in humans. The effectiveness of low-intensity vibration (LIV), which delivers a magnitude of <1 g, has been proven in rats with SCI when applied over 35 days (88). The results of this study showed no change in in the BMD of the distal femur of LIV treated rats compared to a 5% loss in the untreated rats. A study by Davis et al (1) found that the application of WBV (30-50 Hz, 2.16-5.83 g) on an individual with an incomplete SCI for 10 weeks yielded significant positive changes in the BMD in the trunk and spine compared to controls without vibration. The results of this study are promising but require further work to be performed with a larger sample size to verify results.

2.2.8 Health and safety

The negative effects of vibration have been identified in the workplace with vibration related injuries identified in a number of applications including the operators of pneumatic power tools, or drivers of work machines. This has led to legal limits of vibration in the workplace being enforced in many countries (89). There has also been vibration limits placed on commercial WBV training platforms although in Europe these are permitted to exceed the occupational exposure limits provided the exposure is <5 minutes (89).

Typically for training purposes higher magnitudes of WBV are used. In contrast, to avoid risk of injury to older people, vertical vibration is generally applied at low magnitudes. Another health consideration is the substantial amplification of peak accelerations, which arise due to complex interaction of body segment resonances. These have been identified in vertical WBV at frequencies of 10 to 40 Hz and amplitudes >0.5 mm for the ankle (90). Another consideration is the risk of whole body resonant frequencies in vertical WBV which have been identified by Randal et al (91) and found to occur between 9 to 16 Hz. The whole body resonance frequency

poses a risk since this frequency causes a maximum displacement between the organs and skeletal structure, placing strain on the body. Finally, research by Abercromby et al (92) suggest that the risk of adverse health effects may be lower for side-alternating rather than vertical WBV, and for half-squats rather than full squats or upright stance.

Chapter 3: The AnyBody Software

One of the difficulties currently associated with the use of WBV as a rehabilitation intervention for osteoporosis is that its beneficial effects on bone are not yet fully understood. It has already been discussed earlier in the report that the different parameters of WBV studied, such as frequency, amplitude, or platform type, exhibit varying degrees of success depending on a number of aspects of the individual treated, such as their age, gender, and type of osteoporosis they suffer from. One way the effects of different parameters of WBV on the body may be simulated without the requirement for numerous clinical trials is by computational modelling. For this investigation, the computation modelling software chosen was the AnyBody software (93).

3.1 AnyBody overview

The AnyBody software has been developed for the analysis of rigid-body systems, in particular the human musculoskeletal system (94). One of the main advantages of this software is that the body modelled can be subjected to external objects, loads, and motion specifications (94). This has led to the application of AnyBody in research applications in a wide range of fields including sports, gait, aerospace, and orthopaedics (95).

The operation of AnyBody modelling is performed using a text-based input with a special modelling language named AnyScript (94). The completed AnyScript is typically composed of two main sections. The first of these is the model section which contains information of the boundary conditions including the definition of the mechanical system, the body, and the surrounding objects. The second section, the study section, allows a range of analyses and operations to be performed on the model.

3.2 AnyBody Managed Model Repository (AMMR)

The AnyBody Managed Model Repository (AMMR) is a repository of musculoskeletal models available to users of AnyBody. These models originate either from research by academic institutions or collaborations between AnyBody

Technology and academic institutions (96). The two types of models contained in the repository are the body models and the application models.

3.2.1 Body models

The body models are generic models of the body, mostly human although there are also a few animal models. These models serve no function without a context but enable users to analyse a human or animal model without having to create the body model from scratch.

The most widely used model is the AUUHuman, developed at Aalborg University, Denmark (97). This is a fully body model combining body parts developed elsewhere or based on data sets from elsewhere. These body parts have all been connected, with the exception of the mandible model, to create a realistic human model.

3.2.2 Application models

The application models include several example demos created either by users or by AnyBody Technology to demonstrate features of the AnyBody Modelling System (96). These models typically include a body model in some environment or performing some activity. The application section is subdivided into four different folders as illustrated below:

- AnyGait model used to process motion capture data taken in gait labs.
- Validation models used to compare to in vivo measurements
- Example models including models in orthopaedic, rehab, aerospace, and daily activities
- Beta models which have not yet been tested extensively enough to be included with the example models

3.2.3 Scaling laws

One useful feature of the AnyBody human models is the ability to include a custom anthropometric scaling law to scale the model to a specific individual. By default a standard scaling is used for the model which uses the parameters for mass and size roughly corresponding to the 50^{th} percentile European male (98). The first scaling law which can be implemented is “ScalingUniform” which scales defined bone

lengths in three dimensions proportional to their length. Alternatively the size of the bones can be defined not just by the segment lengths, but also by the segment masses to give more accurate dimensions using the "ScalingLengthMass" law. Finally the fat percentage of the body can also be included which can be used to adjust the relative strength of the muscles with the "ScalingLengthMassFat" law. This has an important function in studies of individuals who have conditions which cause muscle atrophy such as multiple sclerosis or SCI.

3.3 Inverse dynamics and muscle recruitment

Anybody uses an inverse dynamics approach to calculate forces on the body based on the kinematics of the body and its inertial properties (94). The principle of this is most easily explained with the use of an example. For the case of a simple arm model shown in Figure 8, the magnitude of the external force, length of the forearm, and insertion point of the muscle on the forearm are all known. From this information it is possible to calculate the muscle force required to balance the moment equilibrium equation about the elbow. Additionally further equilibrium equations can be used to determine the reaction forces at the elbow joint. This is the basis for inverse dynamics.

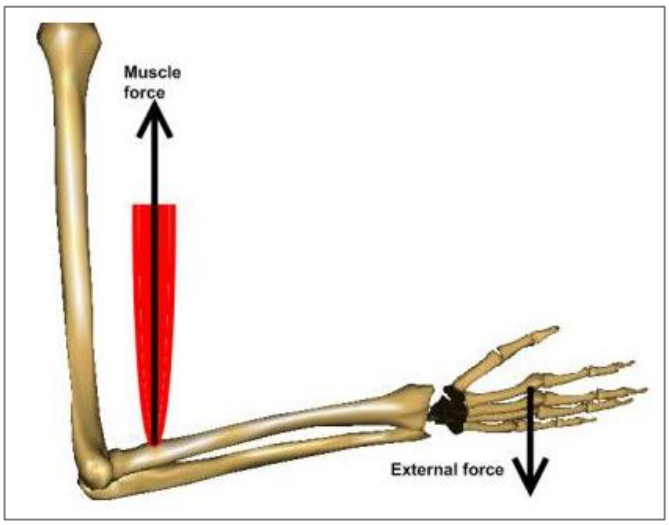

Figure 8: Model of the arm used to illustrate principle of inverse dynamics as performed by AnyBody, taken from AnyBody Technology Inc. (99)

One of the issues faced when solving forces in the body using this method is that the body contains many more muscles than are strictly required to solve these

equilibrium equations. This is turn means that there are infinitely many different ways the muscles can be recruited. In order to overcome this problem, AnyBody handles muscle recruitment using an optimisation calculation. The general form of the optimisation problem is shown in the first part of Equation 2 where G is the objective function, the criterion used to model the muscle recruitment strategy of the central nervous system.

$$\begin{aligned} \underset{f}{\text{Minimize}} \quad & G\left(f^{(M)}\right) \\ Subject\ to \quad & Cf = d \\ 0 \leq f_i^{(M)} \leq N_i, \quad & i \in \left\{1, \dots, n^{(M)}\right\} \end{aligned}$$

Equation 2: Optimisation equation for muscle recruitment in AnyBody, taken from Damsgaard et al (94)

The objective function (G) is a function of the muscle forces $f^{(M)}$ and is minimised with respect to all the unknown forces in the problem, f, which is made up of the muscle forces $f^{(M)}$ and the joint reaction forces $f^{(R)}$. The second part of Equation 2 is the dynamic equilibrium equations which enter as constraints into the optimisation. C is the coefficient-matrix of the unknown forces while d contains the known applied loads and inertial forces. Finally, the non-negativity constraints on the bottom line of the equation stipulate that the all muscles are only able to pull, not push, and the upper boundaries (N_i) limit their capability.

The simplest objective function available is based on the physiological observation that muscles act to limit the metabolic cost involved in the development of a muscle force. This is achieved using a linear objective function and will recruit the minimum number of muscles required to balance the system. This objective function normalises the linear combination of two muscles forces with respect to the strength of the muscles. This maximises the work of strong muscles while weak muscle action is minimised.

The second and most popular optimisation calculation is governed by experimental measurements which show that there is usually more muscle synergy present in generating a muscle force. By allowing more muscle cooperation there is greater

overall muscle strength available and fatigue is preventing by spreading the load over a greater number of muscles. Increased muscle synergy can be simulated in the optimisation calculation by using high order polynomials. The operation of this objective function penalises large terms in the sum which helps distribute the load between more than the minimal number of muscles strictly necessary. Increasing the power of the criterion increases the synergy of the muscles allowing the organism to carry greater loads without overloading the muscles. A drawback of using too high order polynomials is that it may cause activation and deactivations of the muscle which may occur faster that is possible for living muscles. The default criterion for AnyBody is a third order criterion since this is considered a good compromise between different recruitment criteria and suitable for many scenarios.

The final optimisation calculation is the min/max muscle recruitment criteria. This criterion maximises muscle synergy to the extent that the load will be shared as much as possible between the muscles to minimise the maximum load on any one muscle. This means that any activities simulated will not exceed the limit of maximum muscle activity until this becomes absolutely unavoidable. This criterion is essentially a minimum fatigue criterion since the onset of fatigue would occur in the muscle with the maximum relative load. The drawback with this criterion is that muscles which only provide a small positive contribution will activate to their full potential which make give misleading muscle activities. Additionally, as with higher order polynomial criterions, muscle may activate or deactivate faster than physiologically possible

3.4 Measuring muscle activity

The recruitment of muscles to determine the force which they exert has already been discussed. The calculated muscle force is then used to compute the muscle activity by dividing the muscle force by the maximum muscle force the muscle is capable of. In the case of the “simple-type” body muscle model, isometric max voluntary contraction (MVC) is used for all configurations of the model. For the more complex 3-element “Hill-type” muscle model, the strength depends on the muscle length and contraction velocity (100).

As previous mentioned, the AnyBody muscle activity is calculated based on inverse dynamics with a varying degree of muscle synergy considered and does therefore not have a strong biological basis. The determination of muscle activities of using EMG on the other hand has already been discussed and is the complex summation of many motor unit APs. Based on this evidence it is clear that the results of muscle activities measured using these two methods would not be expected to be the same but general trends may be comparable.

3.5 AnyBody studies

In this section a number of previously conducted AnyBody studies will be discussed. The first study has been performed in order to evaluate the similarity between measuring muscle activity using EMG or with inverse dynamics using AnyBody. Subsequent studies demonstrate the feasibility of simulating WBV using the AnyBody software.

3.5.1 Validation of muscle activities

A study which examined the correlation between muscle activities measured using AnyBody and experimentally with EMG has been performed by Zee et al (101). This study compared the EMG activity of a human mandible while performing several tasks, with an AnyBody mandible model performing the same actions with input bite force and kinematics. The study found an average correlation coefficient of 0.580 between these methods of measuring muscle activity and a mean absolute error of 0.109. This correlation coefficient indicates a moderate relationship (102) between muscle activities measured with EMG and with AnyBody.

3.5.2 Whole body vibration studies

The most recent AnyBody study to simulate WBV has been performed by Li et al (103) and investigated the biomechanical response of the musculoskeletal system to WBV in a seated driver model. Inverse dynamics was utilised to analyse a full body musculoskeletal system of a seated individual. Included in the model were rigid bodies of different parts of the car the subject would be in contact with. This model was successfully implemented to determine the muscle activities from vibration at a

range of backrest inclination backrest. Validation of the model was performed using seat-to-head transmissibility and muscle oxygenation of 10 healthy volunteers.

Another study has been conduction by Ma et al (2) into the effects of WBV on humans in different standing postures. A simplified model of the lower limb was subjected to a low magnitude of vibration in order to capture the joint forces and muscle activities. The movements of the lower limbs were captured from a volunteer using Motion Capture System displacement of marked points. Validation of the models prediction of muscle activity was performed from recorded sEMG signals which were measured simultaneously with the motion capture of the individual.

Chapter 4: Methodology

4.1 Designing the model

The first stage of this project was to gain an understanding of the motion of the WBV platform and the effect this had on the human body. This knowledge would be later utilised to develop a computational model which gave a reasonable simulation of WBV.

The primary platform modelled for this project was the Galileo side-alternating vibration plate developed by Novotec Medical (104). The basic operation of this platform has already been discussed and involves side-to-side motion over a central fulcrum, alternately lifting one side of the body while lowering the other (Figure 4, left). This rotation of the platform over the central fulcrum only occurs in one direction and as such rotation can be considered to be zero in the other directions. In addition the central fulcrum of the platform is unable to translate in any direction. Other than the forces from the plate and muscles, the only other significant force which would be expected to act on the body is gravity. From this it can be deduced that there will be a force from the vibration plate pushing each foot upwards alternately but since the foot is not attached to the vibration plate, the only external force pushing the foot back downwards would be the force of gravity.

In order for a comparison between vibration types to be made, a vertical vibration platform was also modelled based on the design of the Power Plate (105) platform. This platform operates by movement of the entire platform upwards and downwards (Figure 4, right). The operation of this platform was easier to design and simply required the platform to be constrained so it could not rotate and only translate in the y direction.

From the descriptions of the two vibration plates it is apparent that each of the plates has only one out of a possible six degrees of freedom (DoF). This is illustrated in more detail in Table 1 where a reference frame is adopted whereby the y-axis points upwards and the z-axis points to the side of the individual.

Table 1: DoF present in each of the two types of vibration platform analysed

Platform Type	Translational DoF	Rotational DoF
Side-alternating	None	z-axis
Vertical	y-axis	None

4.2 Models of whole body vibration

During the course of this investigation, two types of vibration platforms were modelled, side-alternating and vertical WBV. The global reference frame and human body model used in these models are shown in Figure 9 where the obscured vertical axis is the y-axis. All of the simulations designed used the AUUHuman body model from the AMMR. Full details of the major changes in code required to design the platforms is provided in the Appendix. In this section, for each of the models designed, their attributes and their disadvantages will be discussed.

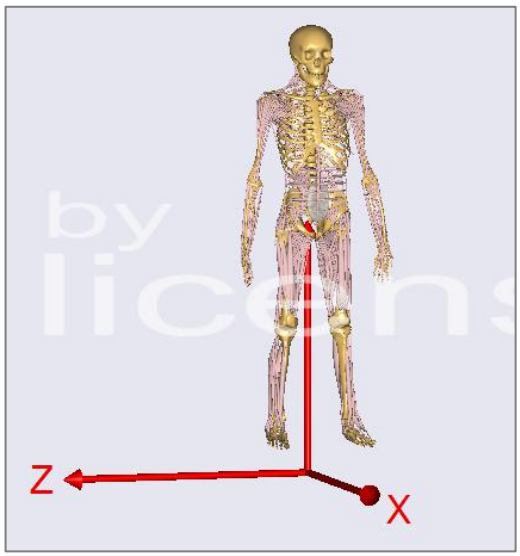

Figure 9: Image of the AnyBody AUUHuman model within the global reference frame

4.2.1 Side-alternating vibration models

The first platform type which was modelled was the side-alternating platform. In the course of designing an accurate simulation, three models of increasing sophistication were designed. The first two models were created to gain a better understanding of the AnyBody software but were considered too flawed to use for the final analysis.

4.2.1.1 Forces only model

The first and most rudimentary model simply involved the application of dynamic forces at the base of the feet intended to approximately simulate those generated during side-alternating WBV. A centre node of each foot was chosen to apply the force using an existing ground joint node as highlighted in Figure 10. Forces of opposite directions were applied to the feet to try to simulate the side-alternating platform which would load one foot while the other was unloaded and vice versa. This was achieved by applying sinusoidal forces to each foot which were 180 degrees out of phase. An image of the analysis using this model with the forces represented by vectors is shown in Figure 11.

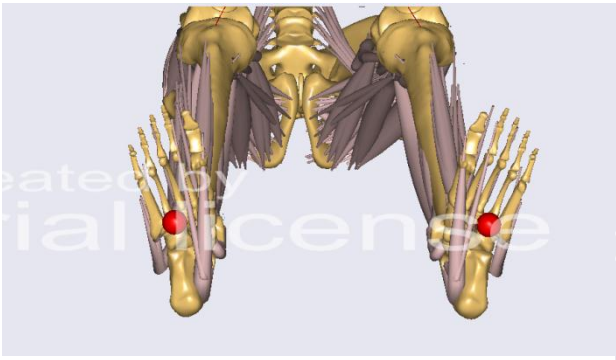

Figure 10: AnyBody model with nodes highlighted at centre of feet

Figure 11: Frontal view of AnyBody model undergoing forces at the nodes

A disadvantage of this model is that it applies the entire force to a single node rather than the whole foot which may not be representative of the force application in side-alternating vibration. Another disadvantage is that an equal positive and negative force is applied to the foot in the y-axis. This is not accurate as the only external negative force in the y-axis exerted on the model should come from the effect of gravity. Finally, this model fails to visualise the motion of the body during loading and as such does not allow the measured muscle activity to be related to body movement.

4.2.1.2 Feet driven by drivers model

The second model was designed to attempt to replicate the actual movement of the body during side-alternating WBV through the use of drivers. To achieve this, linear drivers were attached to the centre nodes of the feet instead of forces. Drivers in AnyBody operate by driving the reference frame of an object w.r.t. another reference frame. In this case the reference frame of the centre node of the foot was driven w.r.t. to the global reference frame in the y-direction. As in the previous model, each foot was driven sinusoidally and 180 degrees out of phase with the other. A screenshot of the model with the global reference frame and nodal reference frame of the foot is shown in Figure 12. Note that in this figure an unrealistically large amplitude of 50 mm is applied to the human model for illustrative purposes to clearly show the elevation and depression of the feet.

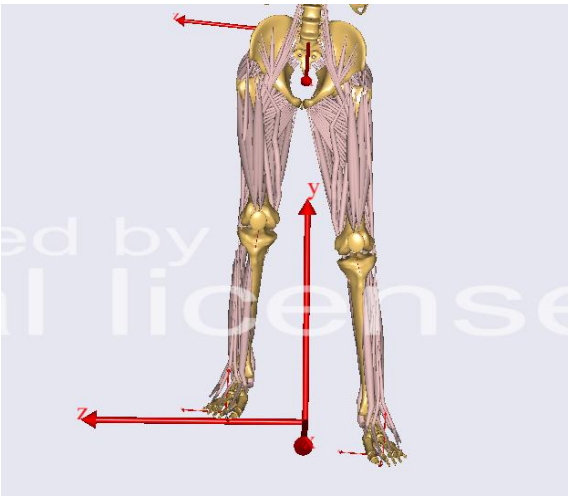

Figure 12: Frontal view of AnyBody model driven by drivers at base of the feet

One disadvantage of this model is that the feet are driven solely in the y direction which would not be the case on either ends of the platform. In reality the tilt of the platform during WBV would be expected to tilt the feet sideways as the body adjusts to maintain balance, causing inversion and eversion of the feet. Additionally, similar to the previous model the feet are driven at an equal acceleration in the positive and negative y-direction which is not realistic.

4.2.1.3 Feet driven by platform model

The final model incorporated the actual platform used in side-alternating WBV in an attempt to achieve more accuracy. The human body was defined relative to the platform by two nodes on each foot, at the heel and at the toe. This is illustrated in a view under the platform in Figure 13 where the red nodes define the position of the feet relative to the platform and the blue node determines the centre of the foot where the amplitude will be calculated.

The platform itself was constrained at a central node using drivers so that no translation and only rotation was in the z direction was enabled. Finally, a rotational driver was specified which would rotate the platform to a certain frequency and to move the feet to a certain amplitude. This was achieved using a sinusoidal function with the desired rotation set as the amplitude and the frequency of the platform set as the frequency of the sinusoid. An image of the model at an amplitude of 10 mm is shown in Figure 14.

In the interests of simplicity a number of variables were arranged so they could be changed simply by altering the mannequin file. This includes the amplitude of the platform at the foot which was subsequently converted to a degree rotation for the rotational driver. This was achieved using trigonometry since the amplitude of the plate and the distance of the feet apart was known. Other variables which could be specified in the mannequin file are the distance of the feet apart, and whether or not the feet were positioned straight or pointing outwards.

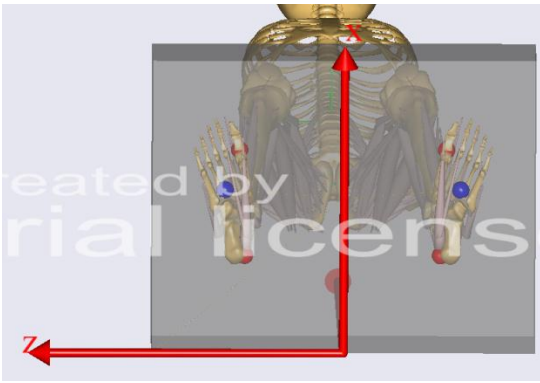

Figure 13: View of feet nodes on AnyBody model from below

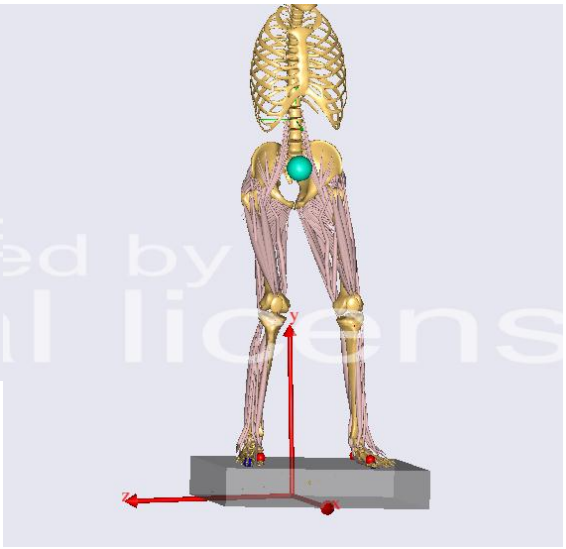

Figure 14: AnyBody model undergoing side-alternating WBV at an amplitude of 10 mm

4.2.2 Vertical vibration model

The second application modelled was the human body on a vertical vibration plate. The vertical vibration plate was created to a similar design as the final side-alternating vibration plate. As previous discussed the main differences between the vertical and side-alternating plates are than the vertical plate contains a centre point with one DoF which is free to move linearly as opposed to rotationally. The consequence of this is the vertical plate must be designed so as to be rotationally fixed. In addition the centre node of the platform had to be changed to allow it to translate linearly in the y direction. Similar to the design of the side-alternating plate, a sinusoidal driver was utilised although it was set to translate the centre of the platform in the y-direction rather than rotate in the z-direction. An image of the model at its maximum and minimum height during a cycle of 20 mm amplitude is shown in Figure 15.

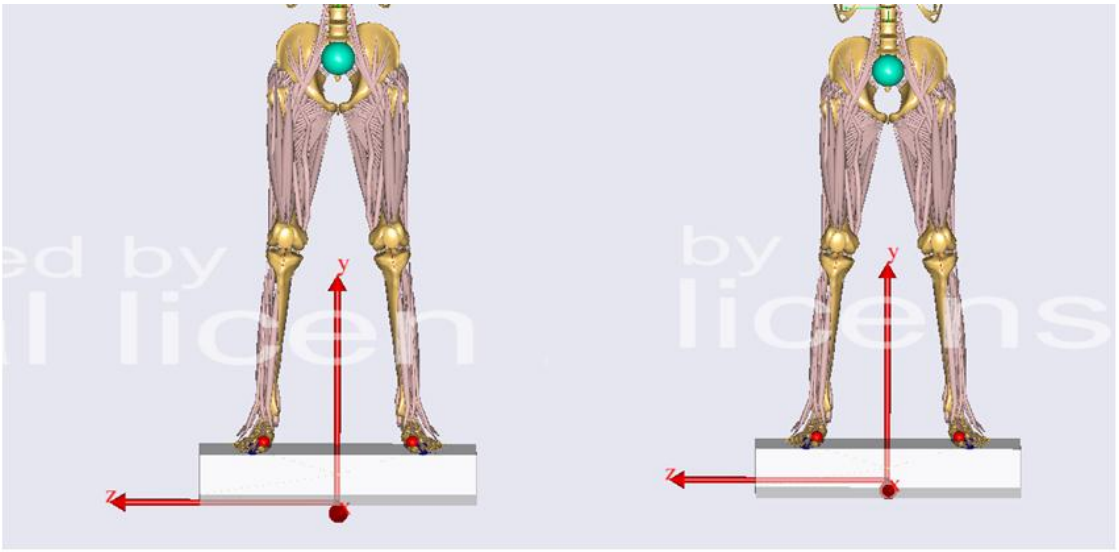

Figure 15: AnyBody model undergoing vertical WBV simulation of 10 mm amplitude at maximum and minimum height respectively

4.3 The human body model

As previously discussed the human body model used for this project was the AUUHuman which is available in the AMMR. By default this body model is positioned in a standing position and has the default scaling. In this section, the alterations which were made to the human model to make it more suitable for the aims of this project will be discussed.

4.3.1 Scaling and defining the human body model

Since this analysis was being designed to achieve results concerning a population of individuals with SCI, as opposed to patient specific data, the standard AnyBody data corresponding to the 50th percentile European male was used. The scaling law used for the analyses was the "ScalingLengthMassFat" law (106) as this enables the fat percentage of the body to be altered with a reciprocal change in the muscle percentage of the model as discussed in a later section.

Final alterations were made to limit the computational time of the analyses. The first of these was to define "simple-type" rather than "hill-type" muscles since the hill muscle type was found to cause an unfeasibly long computational time. Finally the muscles of the arms were not included in the analysis since these were found not to contribute to the muscle activity of the lower limbs of interest.

4.3.2 Body positions analysed

During the course of this investigation the human model was adjusted on the platform to create three different body positions. These were the human model in a squatting (50° knee flexion), knee flexed standing (20° knee flexion), and knee locked standing position (0° knee flexion). For analyses where the body position is not specified, the default body position analysed was the squatting position. All three of the models positioned on the vibration plate are shown in Figure 16. These three positions were chosen to reflect the varying knee flexion of body positions achieved in previous research using WBV interventions. These interventions were mentioned in the background section and involve the individuals with SCI either standing with knee flexed unassisted or with having varying degrees of knee flexion while supported by devices such as tilt tables or standing frames.

In the case of the squatting position and knee flexed standing, approximate values of the measured other joint ankles corresponding to a knee flexion of 50 and 20 degrees respectively were taken from the literature (107). In addition repeated tests were undertaken to see which position minimised muscle activity since it was assumed this position would be preferred by the individual. The final joint angles chosen for the squatting position were hip flexion of 15 degrees, waist flexion of 15 degrees, and ankle flexion of 15 degrees. The knee flexed standing position was designed with hip flexion of 10 degrees, waist flexion of 10 degrees, and ankle flexion of 10 degrees.

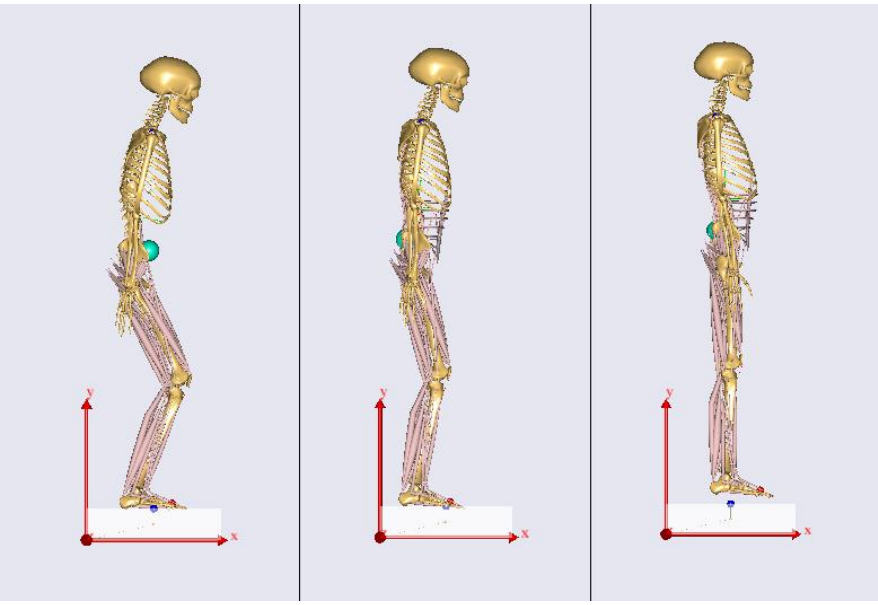

Figure 16: Human body model on WBV platform in three positions: squat (50° knee flexion), knee flexed standing (20° knee flexion), knee locked standing (0° knee flexion)

4.3.3 Simulating spinal cord injury

In order to make this simulation relevant to WBV therapy in individuals with SCI, it was necessary to incorporate the known effects of SCI on the muscles. It has already been established in the background section that individuals with SCI suffer from an average of approximately 15% loss in the muscle mass after injury. The AUUHuman model used in this investigation does not allow the muscle mass percentage to be changed directly and instead calculates this value based on the fat percentage specified. This was incorporated into the model by increasing the body fat percentage with a reciprocal effect of reducing the overall muscle content of the body. The AUUHuman model calculates the mass fraction of muscle (R_{muscle}) left over after considering the mass fraction of fat (R_{fat}) and the mass fraction in the body of organs, blood, skeleton, etc (R_{other}) as illustrated in Equation 3.

$$R_{muscle} = 1 - R_{fat} - R_{other}$$

Equation 3: Length-mass-fat scaling equation (108)

Since the value of R_{other} is fixed ($R_{other} = 0.5$) in the AUUHuman model, it is possible to adjust the value of R_{fat} in order to change the value of R_{muscle}. It was calculated that for the data used for the 50th percentile European male the mass

fraction of fat was $R_{fat} \approx 0.217$. Substituting this value into Equation 3 the default value of R_{muscle} could be calculated:

$$R_{muscle} = 1 - 0.217 - 0.5 = 0.283$$

Subsequently adjusting the mass fraction of muscle to reflect the studies set out in the background which indicates a 15% loss in muscle mass incurred after SCI:

$$R_{muscle} = 0.283 * 85\% = 0.241$$

Finally, since it is not possible to adjust the mass fraction of muscle in the body directly, it was necessary to calculate the mass fraction of fat required to achieve this mass fraction of muscle:

$$R_{muscle} = 1 - R_{fat} - R_{other}$$

$$R_{fat} = 1 - R_{muscle} - R_{other} = 1 - 0.241 - 0.5 = 0.259$$

This is the adjusted value of the mass fraction of fat used to achieve a 15% reduction in the mass fraction of muscles in all of the analyses of this investigation.

4.3.4 Muscles of interest

Since an analysis of every muscle in the lower limbs would be time consuming and difficult to present, it was first necessary to isolate a subset of relevant muscles. As the body positions chosen for the analysis were the squat and variations of standing, the logical muscles to choose were those which have been shown in the literature to be most active in these positions. The muscles active during a squat and standing have already been discussed in relation to the work of Isear et al (6) and Loram et al (5). The squat position was found to show greatest muscle activity in the quadriceps, hamstrings, gastrocnemius, and gluteus maximus, while the standing position stimulated most activity in the soleus and gastrocnemius.

The AnyBody human model is designed so that the musculature is described according to specific muscles rather than muscle groups. For this reason it was more practical to choose to analyse representative muscles rather than their larger muscle group. Muscles were chosen on the basis that they would give an overall picture of

muscle activation in the lower limbs during WBV in both positions. A break-down of the muscles and muscle groups active in the previously mentioned body positions and their function according to literature (3) is shown in Table 2.

Table 2: Muscles involved in squat and standing and their function

Muscle Group	Muscle	Function
Quadriceps	Rectus Femoris	Extension of leg; flexion of thigh
	Vastus Lateralis	Extension of leg
	Vastus Medialis	Extension of leg
	Vastus Intermedius	Extension of leg
Hamstrings	Semitendinosus	Extension of thigh; flexion of leg; medial rotation of flexed leg
	Semimembranosus	Extension of thigh; flexion of leg; medial rotation of flexed leg
	Biceps Femoris	Extension of thigh; flexion of leg; lateral rotation of flexed leg
Others	Gluteus Maximus	Extension, lateral rotation, abduction, and adduction of thigh
	Gastrocnemius	Plantar flexion of foot; flexion of leg of free limb
	Soleus	Plantar flexion of foot

For the AnyBody simulations, the subset of five muscles selected were the rectus femoris (RF), vastus lateralis (VL), biceps femoris (BF), gluteus maximus (GM), and gastrocnemius (GN). An overview of these muscles origin and insertion points gathered from the literature (3) is outlined in Table 3.

Table 3: Selected muscles and their origin and insertion points

Muscle	Origin Point	Insertion Point
Rectus Femoris (RF)	Anterior inferior Ilium	Proximal end tibia
Vastus Lateralis (VL)	Proximal end femur	Proximal end tibia
Biceps Femoris (BF)	Ischium and shaft of femur	Proximal end fibula and proximal end tibia
Gluteus Maximus (GM)	Ilium, sacrum and coccyx	Proximal end femur
Gastrocnemius (GN)	Distal end femur	Heel bone

4.4 Analysis

4.4.1 Data collection and processing

All analyses were performed to calculate either the muscle activity or muscle forces as determined using inverse dynamics with the AnyBody software. A third order polynomial optimisation criterion was chosen for muscle recruitment since this would produce plausible muscle synergy and realistic muscle activation and deactivation frequencies. The duration of the analysis in all cases was a period of 1 second since this was judged be sufficient time to study the behaviour of the muscles. Analyses were performed only of the right leg since the model gave identical results for both legs albeit with a phase shift of 180 degrees in the case of the application of side-alternating WBV. Muscle activities and forces are either presented as the mean or peak of the overall recording with respect to the time measured. This is illustrated in Figure 17 for the RF muscle with the squat body position under side-alternating WBV of 20 Hz and 1 mm. The peak muscle activity (green line) and mean muscle activity (red line) measured over the entire recording of muscle activity (blue line) are highlighted.

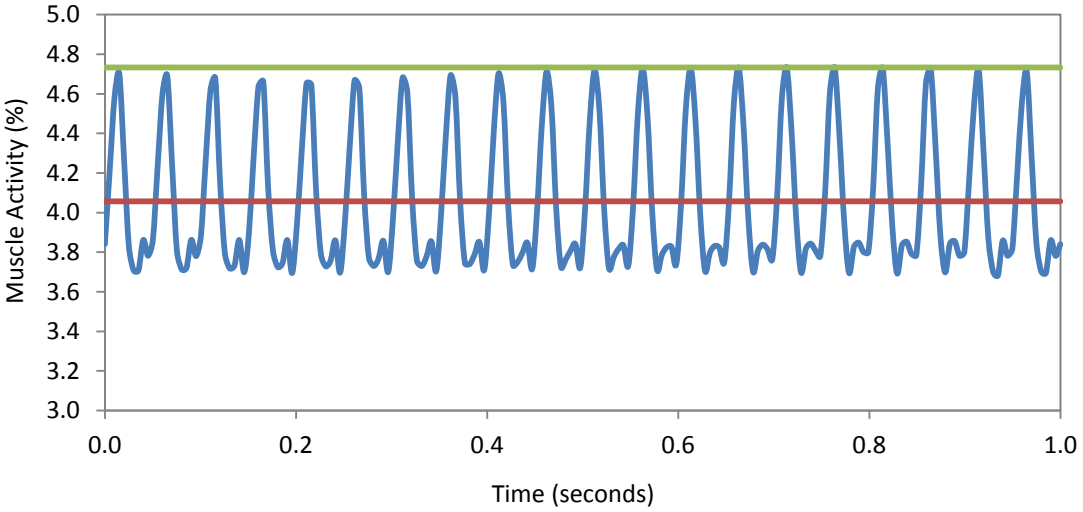

Figure 17: Muscle activity of the rectus femoris muscle measured during WBV of 20 Hz and 1 mm. Represented are the time varying muscle activity (blue line), max muscle activity recorded (green line), and mean muscle activity recorded (red line)

For instances where the muscles of interest were split into several fibres in the AUUHuman model, additional work was needed to calculate data for the overall muscle. In the case of calculating overall activity of the muscle an average was taken across the muscle fibres in an attempt to replicate the measurement of sEMG which takes a weighted average of the motor units. Subsequently the muscle activities were converted to a percentage before plotting. The overall force of the muscle was calculated by taking the summation of all the muscle fibres since these would all contribute to creating the force of the muscle. Muscle forces were then converted from their default value as a force in all three component directions to the overall magnitude before plotting.

4.4.2 Parameters studied

During the course of this investigation a number of WBV parameters were tested and the respective muscle activities or forces measured. In order to make the simulations as realistic as possible, frequencies and amplitudes chosen for the applied WBV were taken from within the achievable limits set out by the manufacturers of the vibration plates simulated as shown in Table 4.

Table 4: Comparison of different vibration types (109)

Platform Type	Frequency Range	Amplitude Range
Side-alternating (Galileo)	5-30 Hz	0-4.5 mm
Vertical (Power Plate)	25-50 Hz	1 or 2 mm

The aim of the first analysis was to study the effect of body position without WBV on the activation of selected muscles of the lower limbs. This was performed in order to get values of the normal mean muscle activities which could then be compared to values taken with the application of WBV. A subsequent analysis of the different body positions with WBV was simulated at a frequency of 20 Hz and 1 mm.

Although this had already been incorporated into the previous analysis, the next stage of the investigation was to determine what effect simulating SCI by adjusting the muscle mass fraction had on the overall muscle activities. This was performed by comparing the mean muscle activities of the reduced muscle mass human model with the human model with average muscle mass.

The next stage was to investigate the effect of a number of different WBV parameters on muscle activities of the human body in a squatting position. The first parameter analysed was the effect of different vibration types by comparing the effects of side-alternating and vertical vibration plates on mean muscle activity of the human body squatting model. The frequency and amplitude were chosen within the values which were achievable using both platform types as defined in Table 4. The selected values which overlapped between the platform types were a frequency of 30 Hz and amplitude of 2 mm. The subsequent parameters analysed were the effects of frequency and amplitude of the side-alternating WBV platform on the mean muscle activities. Frequencies and amplitudes were again chosen from within the achievable limits set out for the side-alternating WBV specified in Table 4. Frequencies were chosen between 10 and 30 Hz and amplitudes between 1 and 3 mm.

Having gathered muscle activities under a range of parameters, the next stage of the analysis was to see whether a similar trend could be observed for muscle forces. In order to allow a comparison to be made between mean muscle activities and forces, the same squatting body position and side-alternating WBV plate were simulated.

The difference between this analysis and the previous is that muscle forces were assessed at configurations which increased frequency and amplitude simultaneously. The four configurations tested were (i) no WBV, (ii) WBV of 10 Hz and 2 mm, (iii) WBV of 20 Hz and 3 mm, and (iv) WBV of 25 Hz and 3.5 mm. Muscle forces were presented both as mean and peak values for comparison purposes.

The final analysis was to compare the patterns of muscle activity of the RF before and after the application of side-alternating WBV of 10 Hz and 2 mm. The purpose of this analysis was to better understand how the patterns of muscle activities change with and without the application of WBV in this AnyBody analysis.

Chapter 5: Results

5.1 Mean muscle activity of various body positions

In this section a comparison was made between the effects of no WBV and side-alternating WBV at a frequency of 20 Hz and amplitude of 1 mm, on the mean muscle activities of the chosen body positions.

5.1.1 No WBV

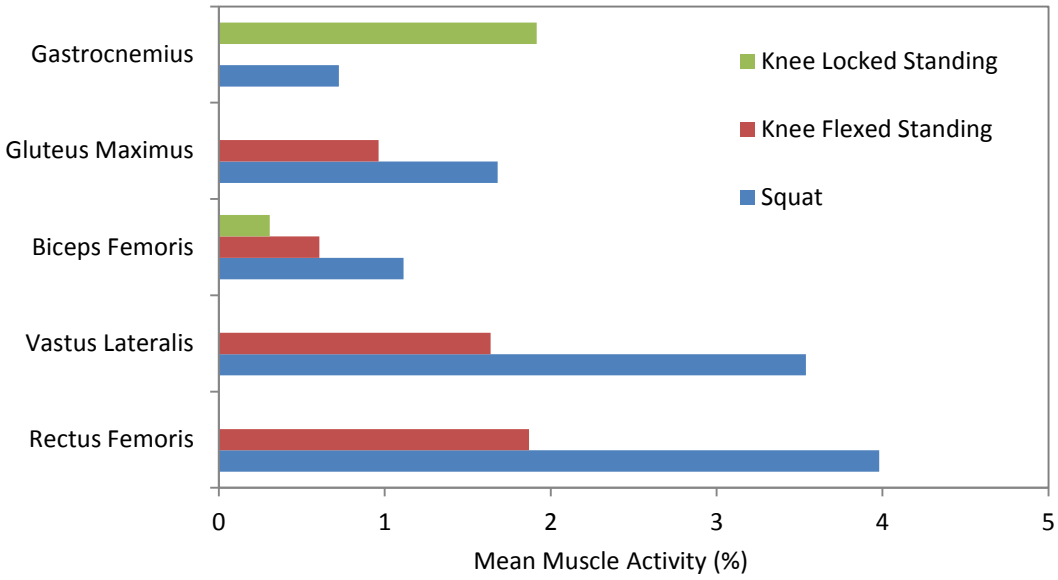

Figure 18: Mean muscle activities recorded by muscles of the lower limbs of different static body positions of the human body

The mean muscle activities produced in the three body positions simulated are displayed in Figure 18. This figure demonstrates that as expected the mean muscle activity varies greatly between the different body positions without the application of WBV.

The squat position shows a high level of muscle activation in the RF (4%) and VL (3.5%) of the quadriceps compared to the BF (1.1%) of the hamstrings. In addition there is a considerably muscle activity shown by the GM (1.7%) and the least amount of muscle activity shown by the GN (0.7%).

The knee flexed standing position showed similar muscle activity to the squat position but at a reduced magnitude. Similar to the squat position the greatest muscle activity occurs at the RF (1.9%) and VL (1.6%). Additionally there is activity at the GM (1%) and BF (0.6%) but virtually no activity at the GN.

Finally, the knee locked standing position shows muscle activities which vary greatly from the other two positons. This includes a highest mean muscle activity at the GN (1.9%) which is least active in the other two body positions. In addition, there is virtually no activity in the muscles of the quadriceps (RF and VL) and GM but there is a small amount of activity at the BF (0.3%) of the hamstrings.

5.1.2 WBV

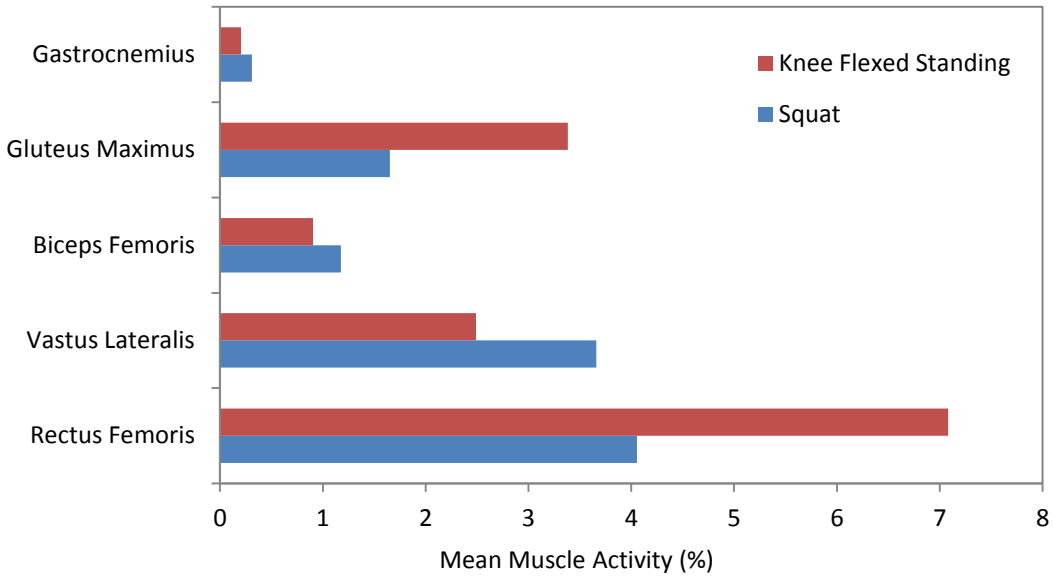

Figure 19: Mean muscle activities recorded by muscles of the lower limbs of different body positions of the human body model undergoing side-alternating WBV of 20 Hz and 1 mm amplitude

The results of Figure 19 indicate that after the application of side-alternating WBV of frequency 20 and amplitude 1 mm, there is a large change in the mean muscle activity of some of the body positions.

A comparison of the results of mean muscle activities for the squat position with and without the application of WBV shows a relatively small change in the mean muscle activities. This is evidenced by a largest increase in muscle activity of the muscles analysed shown by the BF of just 1.1 times compared to without WBV.

In contrast, the knee flexed standing body position shows a far greater change mean muscle activity. This includes muscle activities of the RF (7.1%) and GM (3.4%) compared to values without the application of WBV of RF (1.9%) and GM (1%) an increase of over 3 times compared to without WBV.

Finally, an analysis of the standing with knee locked standing position resulted in muscle activities which increased to such an extent with the application of WBV that they exceeded the upper boundary set by AnyBody. This indicates that these muscle activities exceeded the feasible limits achievable by the human body modelled and as a result cannot be displayed.

5.2 Mean muscle activity of SCI vs no SCI

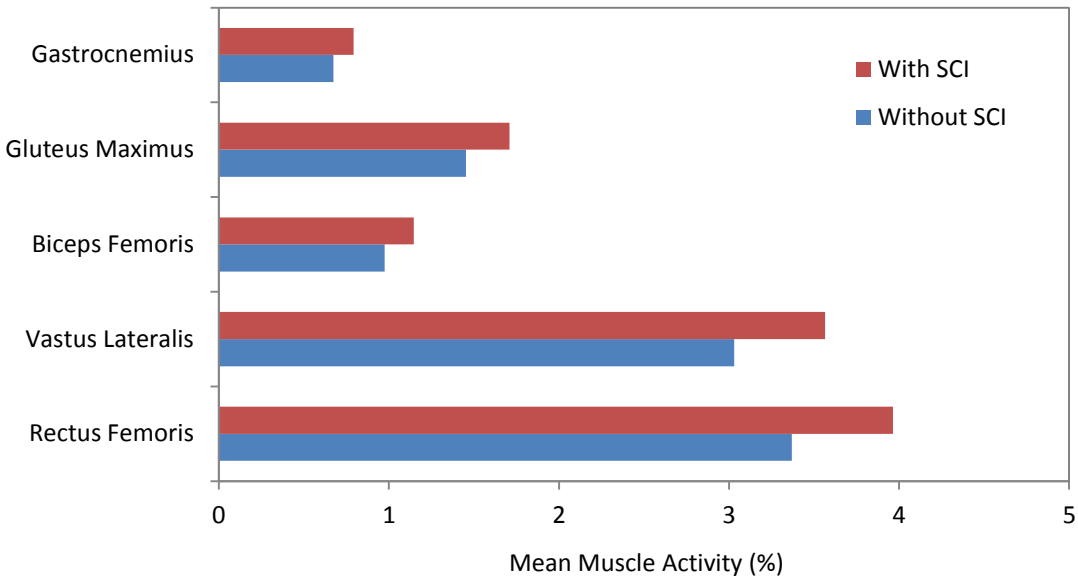

Figure 20: Mean muscle activities recorded by muscles of the lower limbs comparing two models in a squatting position, one including the simulation of SCI and the other not

An analysis of the effect of simulating SCI in the human body model by reducing the muscle mass percentage is shown in Figure 20. This figure demonstrates that the effect of simulating SCI is an overall increase in mean muscle activity compared to the model of a healthy individual. An increase in mean muscle activity of 1.18 times was measured for all muscles analysed for the SCI compared to the non SCI model. This result is logical when considering that a smaller muscle mass would require

greater muscle fibre recruitment, and hence muscle activity, to achieve the same muscle force to maintain the body position.

5.3 Mean muscle activity under WBV parameters

At this stage of the analysis the mean muscle activity of the squatting position was assessed under varying parameters of platform type, frequency and amplitude.

5.3.1 Vibration type

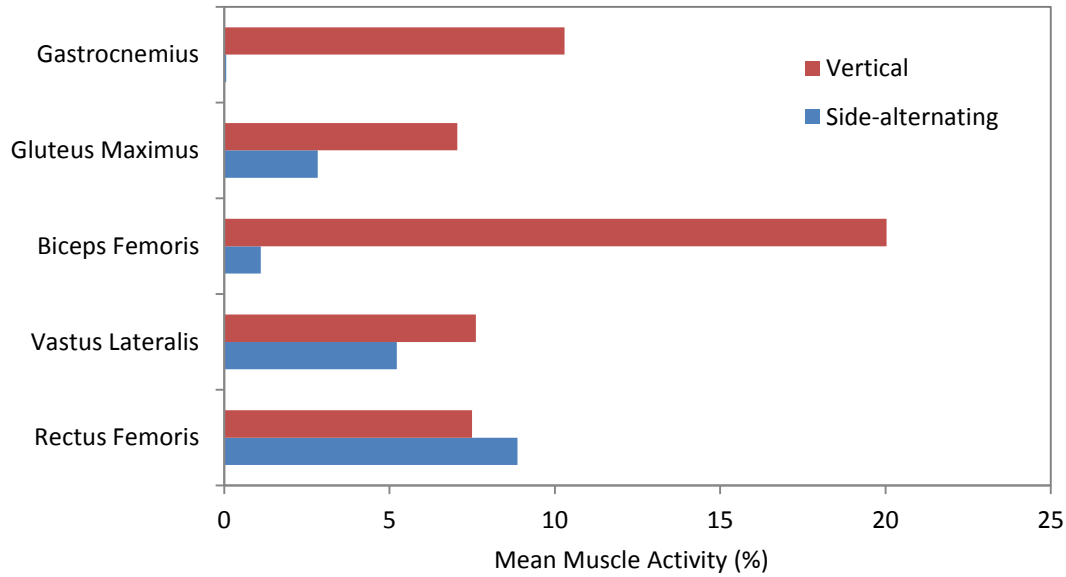

Figure 21: Mean muscle activities recorded by muscles of the lower limbs of a squatting human body model undergoing 30 Hz and 2 mm WBV

The effect of different vibration types at frequencies of 30 Hz and amplitude 2 mm on mean muscle activity in the squatting position are shown in Figure 21. These results demonstrate that the vibration type has a great effect on the overall mean muscle activity. This effect is best illustrated by comparison with the results of mean muscle activity of the squatting position without the application of WBV, as shown in Figure 18, which displayed lowest muscle activities for the GN (0.7%) and BF (1.1%) muscles.

Comparing these activities after the application of 30 Hz and 2 mm side-alternating vibration, there is virtually no change or a reduction in recorded muscle activities of the GN and BF which recorded ≈0% and 1.1% respectively. Other muscles which already fairly active without WBV however increase substantially in activity with the

application of side-alternating WBV such as increases in muscle activity of the RF (2.2 times) and VL (1.5 times).

In contrast the increases in muscle activity seen by vertical vibration at the same specification are generally much larger and show large increases in muscles which had virtually no activity without the application of WBV. This is shown by muscle activities of the GN (10.3%) and BF (20%) after vertical WBV which are 14.2 times and 18 times greater than the muscle activities recorded without WBV. In addition to this, greater muscle activities are shown for vertical WBV than side-alternating in the muscles of the VL (7.6%) and GM (7.1%) but not in the RF (7.5%).

5.3.2 Frequency and Amplitude

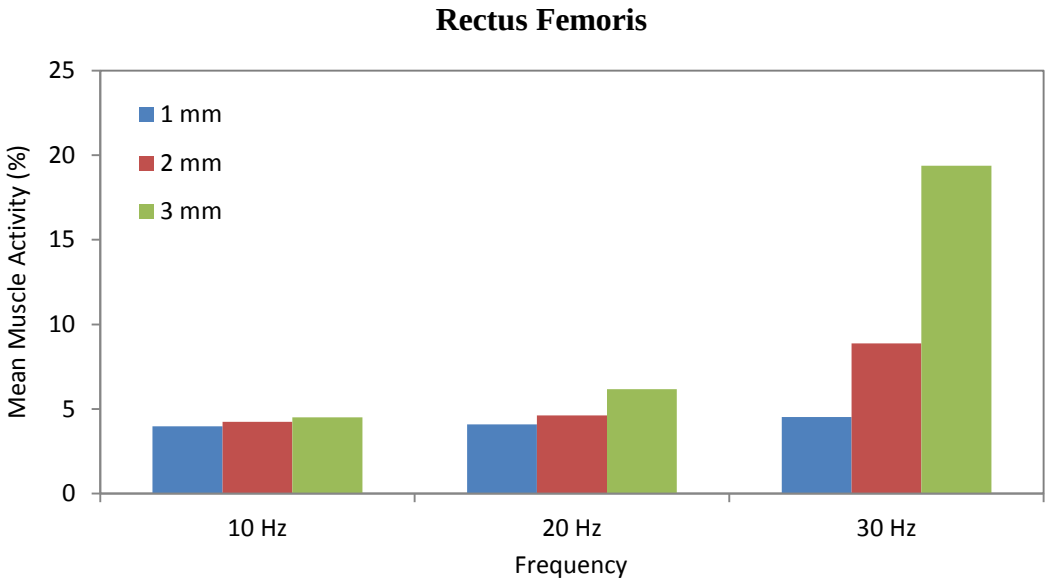

Figure 22: Mean muscle activities recorded of the rectus femoris of a squatting human model undergoing side-alternating WBV at a range of frequencies and amplitudes

The results of Figure 22 illustrate that the frequencies and amplitudes tested have a positive effect on the muscle activities of the RF. At low frequency and amplitude (10 Hz, 1 mm) there is no increase in muscle activity compared to no WBV (4% with and without WBV). This muscle activity does however increase at higher amplitudes (10 Hz, 3 mm) to 4.5%. A similar trend is shown at a higher frequency of 20 Hz with a greater mean muscle activity at higher amplitudes (20 Hz, 3 mm) of 6.2%. Finally, the greatest mean muscle activity of 19.4% is shown at the highest frequency and

amplitude tested (30 Hz, 3 mm) which is 4.85 times the mean muscle activity without WBV. Overall these results show that a combination of high frequency and high amplitude are required to achieve high mean muscle activities at the RF during squatting.

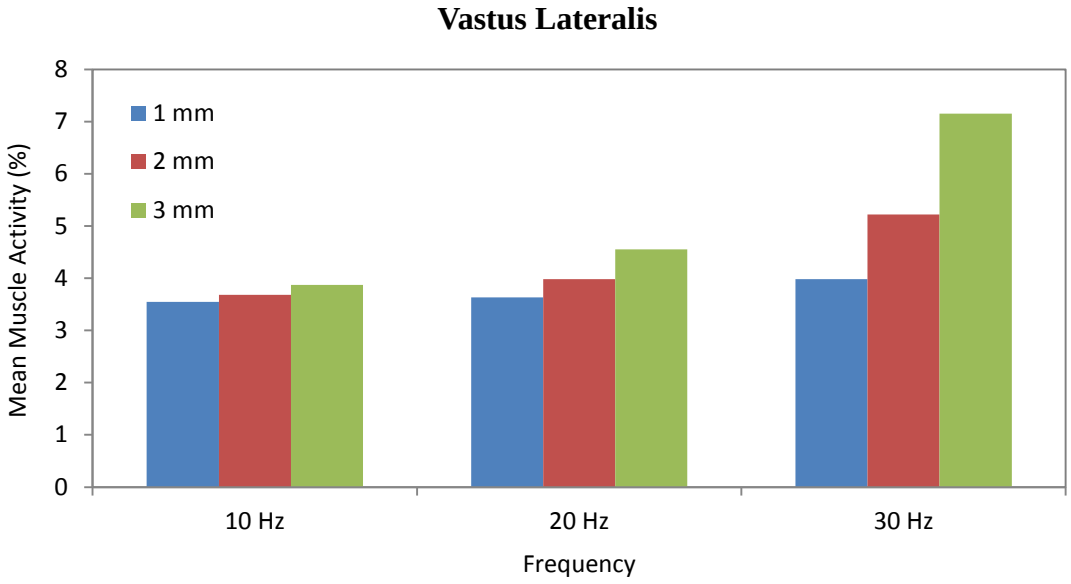

Figure 23: Mean muscle activities recorded of the vastus lateralis of a squatting human model undergoing side-alternating WBV at a range of frequencies and amplitudes

The results of Figure 23 show that, similar to the response of the RF, there is a positive effect of all frequencies and amplitudes of WBV tested on the mean muscle activities of the VL. At low frequency and amplitude WBV (10 Hz, 1 mm) there is no change in mean muscle activity (3.5% with and without WBV) although this increases at higher amplitudes (10 Hz, 3 mm) to 3.9%. A positive trend of muscle activity is shown with the parameters with a higher frequency and same amplitude (20 Hz, 3 mm) resulting in a mean muscle activity of 4.6%. Finally the largest mean muscle activity produced at the highest frequency and amplitude (30 Hz, 3 mm) is 7.1% which is 2 times greater than without WBV. Overall these results show a positive increase in mean muscle activity at all frequencies and amplitudes tested for the VL.

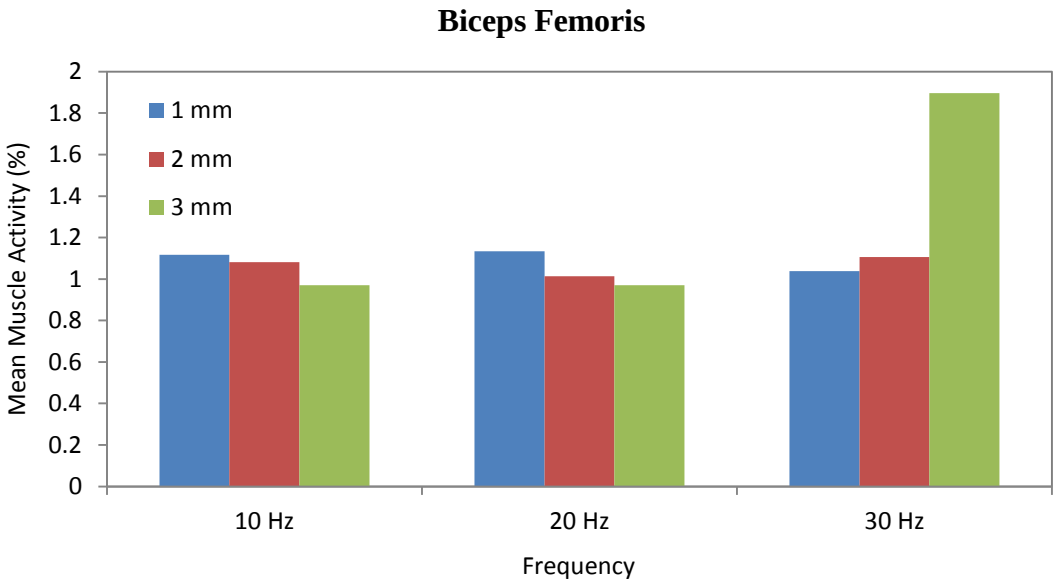

Figure 24: Mean muscle activities recorded of the biceps femoris of a squatting human model undergoing side-alternating WBV at a range of frequencies and amplitudes

The trend of mean muscle activities recorded of the BF, shown in Figure 24, differ from the previous muscles analysed with varying effect of the frequencies and amplitudes tested on mean muscle activity. At a low frequency and amplitude (10 Hz, 1 mm) the mean muscle activity shows no change compared to without WBV (1.1% with and without WBV). The effect of increasing the amplitude at 10 Hz has a negative effect on the mean muscle activity with muscle activities at 2 mm (10 Hz, 2 mm) of 1.08% and 3 mm (10 Hz, 3 mm) of 0.97%. This trend of amplitude having a negative effect on the mean muscle activity is repeated at 20 Hz but not at the higher frequency of 30 Hz. This is illustrated at the highest amplitude at this frequency (30 Hz, 3 mm) which show a mean muscle activity of 1.9%, 1.7 times greater than without WBV. Overall these results show little or no effect of frequency and a negative effect of amplitude on mean muscle activity up until a frequency of 30 Hz where there is also a positive effect of amplitude.

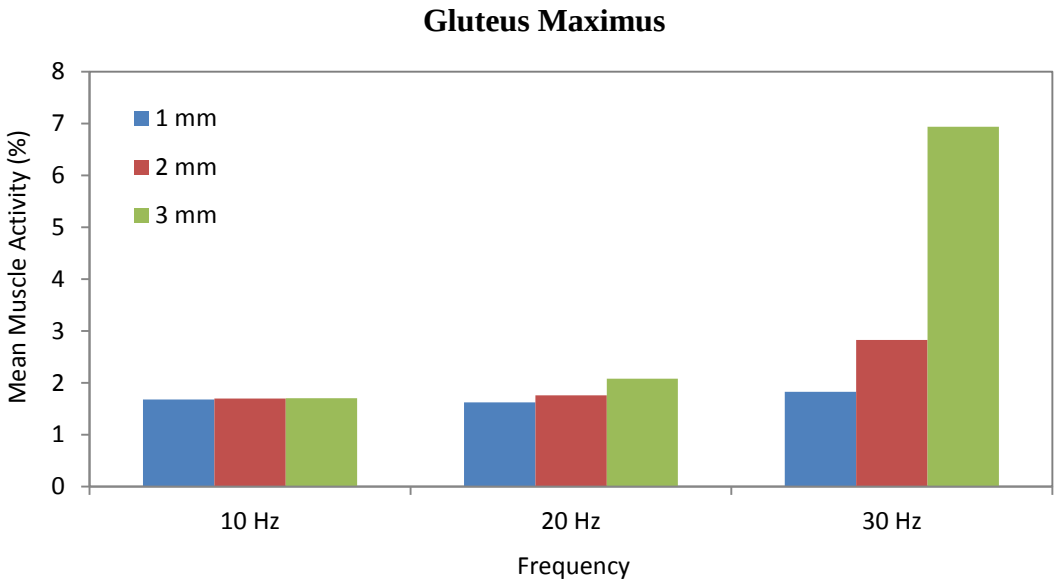

Figure 25: Mean muscle activities recorded of the gluteus maximus of a squatting human model undergoing side-alternating WBV at a range of frequencies and amplitudes

The results of Figure 25 show that there is a positive effect of the frequencies and amplitudes tested on mean muscle activity which becomes more pronounced at higher frequencies. At low frequency and amplitude (10 Hz, 1 mm) there is no effect of WBV on the mean muscle activity (1.7% with and without WBV). Increasing the amplitude at this frequency (10 Hz, 3 mm) similarly causes no change in this muscle activity. The effect of increasing the frequency alone (20 Hz, 1 mm) actually causes a decrease in mean muscle activity (1.6%) although this increases at higher amplitudes (20 Hz, 3 mm) to 2.1 %. At the highest frequency tested and lowest amplitude (30 Hz, 1 mm) there is shown to be an increase in muscle activity to 1.8%. An increase of amplitude at this frequency (30 Hz, 3 mm) results in the highest recorded muscle activity of 6.9% which is 4.05 times greater than without WBV. Similar to the BF, these results shows no effect of frequency and little effect of amplitude on the mean muscle activity up until a frequency of 30 Hz.

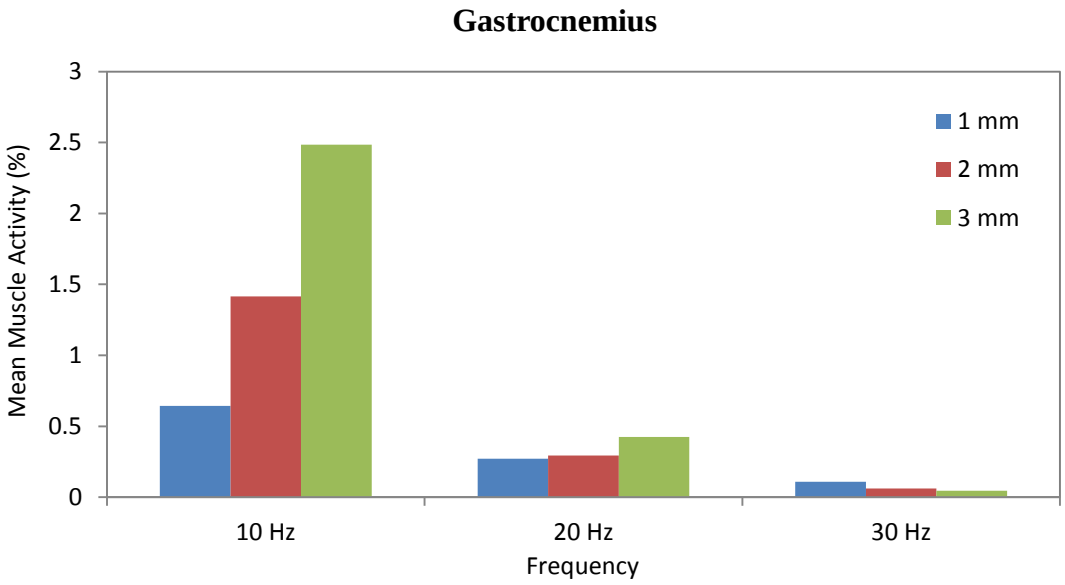

Figure 26: Mean muscle activities recorded of the gastrocnemius of a squatting human model undergoing side-alternating WBV at a range of frequencies and amplitudes

The results of Figure 26 show results of the effects of the tested frequencies and amplitudes on the mean muscle activity of the GN contrast those of previous muscles analysed. At a low amplitude and frequency (10 Hz, 1 mm) there is a reduction in muscle activity compared to the no WBV condition (0.7% without WBV compared to 0.6% with WBV). This value increases with amplitude however to 1.4% (10 Hz, 2 mm) and 2.5 % (10 Hz, 3 mm). This effect is not replicated at higher frequencies which show a large reduction in mean muscle activity. For instance at higher frequencies muscle activities were recorded of just 0.4% (20 Hz, 3 mm) and ≈0% (30 Hz, 3 mm). Overall these results show that the mean muscle activities peak at a frequency at 10 Hz and then decline at subsequent increments. Finally, the amplitude of vibration is shown to have a positive effect on mean muscle activity at 10 Hz and 20 Hz but not 30 Hz. The maximum mean muscle activity recorded (10 Hz, 3 mm) is 3.6 times greater than the condition without WBV.

5.4 Muscle forces under WBV parameters

The next stage of the investigation was to analyse how both the mean and peak muscle forces changed under a variety of amplitude and frequency WBV specifications.

5.4.1 Mean muscle forces

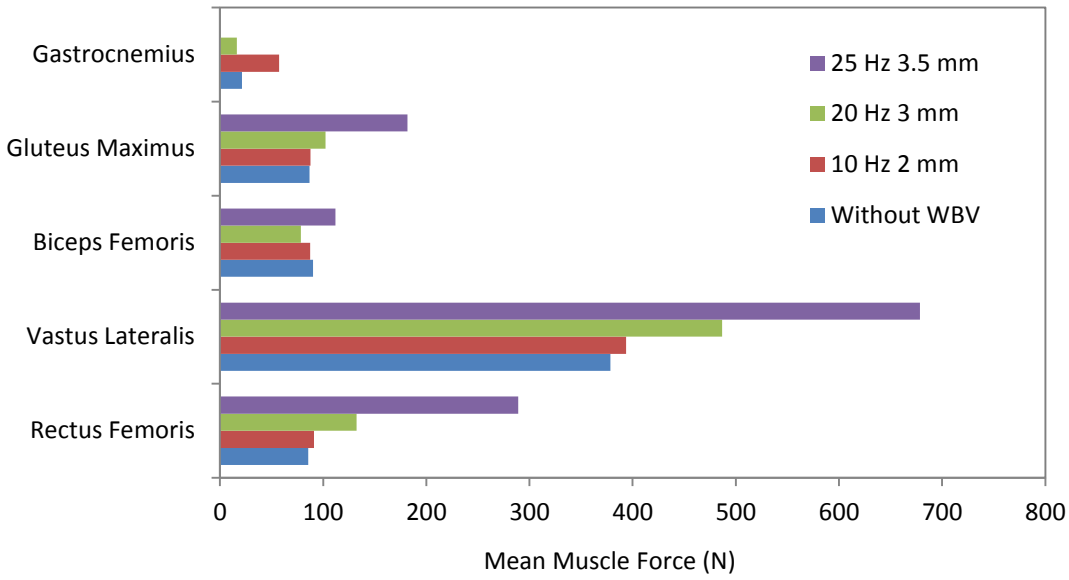

Figure 27: Mean muscle forces recorded by muscles of the lower limbs of a squatting human model with and without the application of side-alternating WBV

Figure 27 illustrates that several different specifications of side-alternating WBV have a large effect on the mean muscle forces produced compared to without WBV configuration in the squatting position. The results without WBV show that the greatest muscle forces are exhibited at the VL (379 N). Three other muscles are shown to exert similar forces, the BF (90 N), GM (87 N) and BF (85 N) while the GN produces just 21 N.

The simulation of the first specification of WBV (10 Hz, 2 mm) shows only a small increase in the mean force produced by some muscles compared to without WBV. The mean muscle force of the RF increases by 1.1 times compared to the non-WBV condition while the muscles of the VL and GM increase by just over 1 times. The second set of parameters of WBV (20 Hz, 3 mm) shows an further increase in three of the muscles with a maximum increase of 1.5 times of the RF compared to the non-

WBV condition. The final set of WBV parameters (25 Hz, 3.5 mm) continues this trend with an increase of the RF of 3.4 times compared to the non-WBV condition and resulting in a mean muscle force of 291 N.

These results of mean muscle forces general replicate the pattern shown by mean muscle activity as expected. The muscles of the VL, RF and GM similarly show a positive effect of frequency and amplitude on mean muscle forces. In addition the BF only increases in mean muscle forces at higher frequencies while the GN shows a negative effect of frequency on mean muscle forces after 10 Hz. The muscle which showed greatest change in mean muscle activity, the RF, similarly showed the greatest increase in mean muscle force as expected while the highest mean muscle force was recorded by the VL at 686 N.

5.4.2 Peak muscle forces

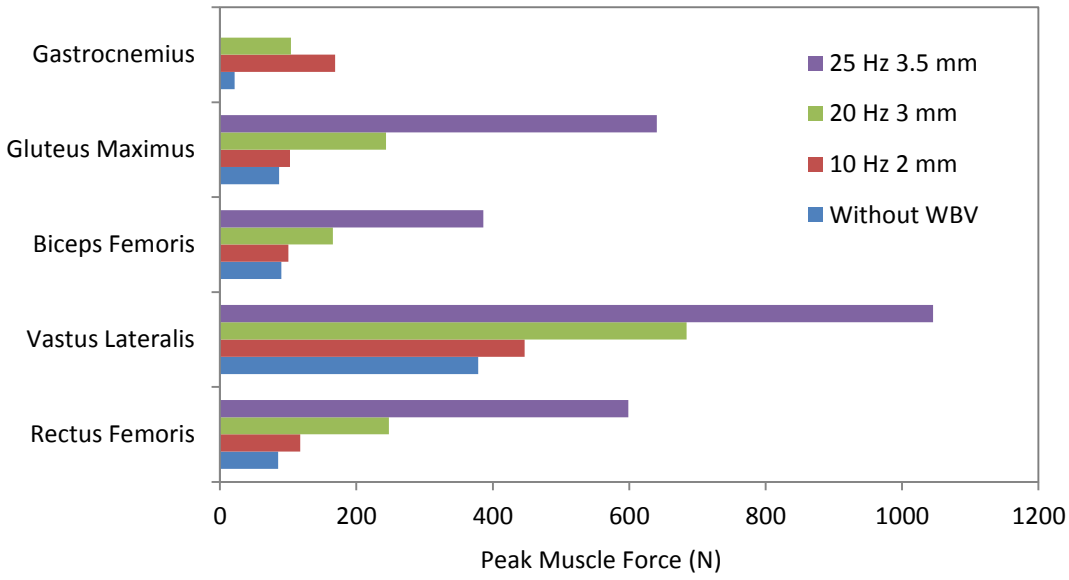

Figure 28: Peak muscle forces recorded by muscles of the limbs of a squatting human body with and without application of WBV

The results of peak muscle forces, shown in Figure 28, at the same specifications of side-alternating WBV simulated previous indicate that the peak muscle forces do not necessarily follow the same trend as the mean muscle forces. The first specification of WBV (10 Hz, 2 mm) which resulted in little no change in mean muscle in the previous analysis can be seen to cause a sizable change in the peak muscle forces in

those same muscles. This is evidenced by an increase in the peak muscle forces compared to the no WBV condition of the RF, VL, and GM of 1.4 times, 1.2 times, and 1.2 times compared to the increase in mean muscle forces of the same muscles which are 1.1 times, 1 times, and 1 times respectively. In addition to this, the peak forces at all the WBV parameters are substantially greater than the mean forces, as shown at the final WBV parameter (25 Hz, 3.5 mm) which shows a peak muscle force of 1045 N compared to a mean force of 678 N for the VL. Finally the diagram of peak forces shows that although the BF does not exhibit a sizable change in mean forces under increasing frequency and amplitude, it does however an increase in peak forces with an increase of 1.8 times with WBV (20 Hz, 3 mm) compared to without WBV. This is further increased to a 4.3 times increase at WBV of 25 Hz and 3.5 mm amplitude.

5.5 Patterns of muscle activity

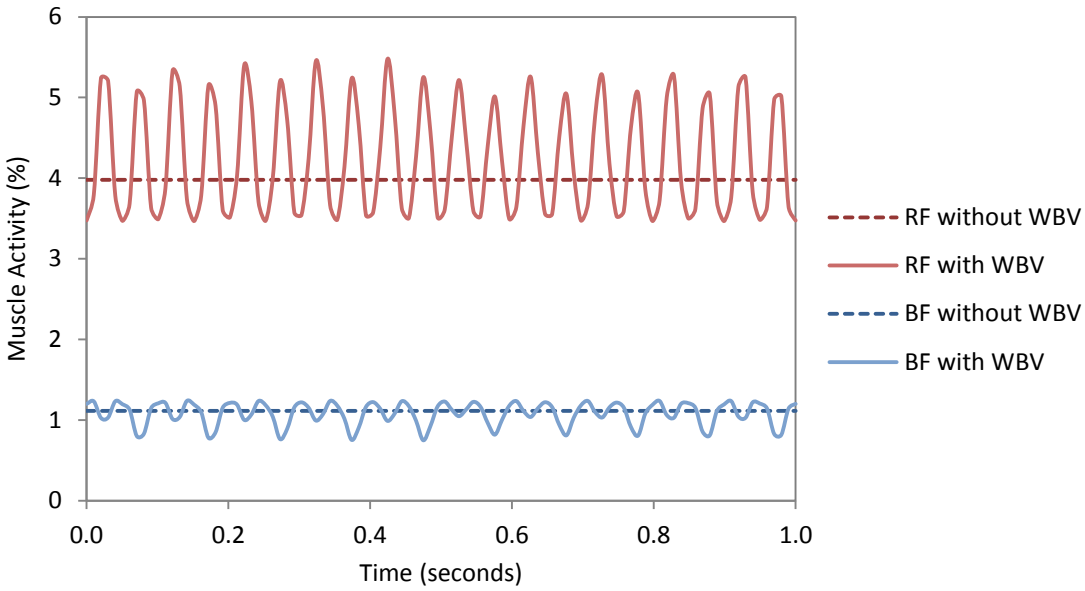

Figure 29: Muscle activity of the rectus femoris and biceps femoris muscles with and without the application of WBV of 10 Hz and 2 mm amplitude

One of the significant differences observed in the diagrams of mean and peak forces of Figure 27 and Figure 28 is that while the mean and peak forces of the squat without WBV are identical, the mean and peak forces with WBV vary significantly. This can be explained by examining the pattern of muscle activity of two muscles, the RF, and BF as shown in Figure 29. This figure shows that for a static movement

such as holding a squat, AnyBody considers the muscle activity to be constant and as such the mean and peak forces are identical. The results of the squat with the application of WBV (10 Hz, 2 mm) on the other hand show muscle activity which oscillates sinusoidally. This explains why the peak muscle forces with WBV are greater than the peak muscle forces without WBV even when the mean forces of the same specification are similar.

Chapter 6: Discussion

The objective of this report was to develop a computational model of WBV intervention in an individual with SCI in order to better inform the treatment of osteoporosis associated with this condition. By analysing the muscle activation and forces developed under a variety of WBV parameters it was hoped that the computational model could be used to inform which muscles create the greatest load on the bones under different parameters. This information could in turn be used for targeted loading of specific bones with WBV in individuals with SCI depending on where their bone loss is most pronounced. In this section the results of the investigation will be discussed w.r.t. the wider findings of the literature. Secondly, the limitations of the investigation will be analysed as well as any future work which could be performed.

In order for the results of the simulation to be discussed in relation to those of the literature, it is first important to highlight the possible errors associated with this comparison. The most obvious limitation was that mathematically derived muscle forces were recorded using AnyBody whereas the medium most often used to measure muscle activity in experimental studies is sEMG. The similarity of these mediums has already been discussed through the work of Zee et al (102) which found an average correlation coefficient between these methods of 0.580. This result indicates only a moderate relationship between these methods which suggests there may be limitations in the use of EMG data to validate muscle activities determined using AnyBody. A second issue encountered was that published papers varied extensively in the WBV parameters used, such as vibration type or frequency, and as such it was not always possible to make comparisons between the literature and simulation at the same parameters. A final limitation was that often studies only reported the muscle activities measured with the application of WBV without measuring baseline readings before the application of WBV. This meant that there were only a limited number of studies with which the effect of WBV against no WBV could be compared to the results of the simulation.

6.1 Muscle activity

The first section of the analysis was principally to attempt to validate the model by comparing the trend of muscle activities measured during the simulation with EMG data at similar vibration parameters in the literature. The second aim was to understand how the muscle activities changed under varying WBV parameters in order to understand the magnitude with which underlying bones would be loaded.

6.1.1 Comparison with experimental work

The first analysis conducted was a comparison of the effect of body position on the muscle activity with and without WBV. The results of mean muscle activities of the squat position without WBV, shown in Figure 18, revealed the greatest muscle activity in the RF and VL of the quadriceps, followed by smaller but significant muscle activities at the GM, BF of the hamstrings, and GN. For the second body position, the knee flexed standing position, the amount of knee flexion was reduced. This position was found to produce similar muscle activities but at a reduced magnitude, other than the GN which showed virtually no muscle activity. Finally the knee locked standing position, with no knee flexion, showed no activity in the quadriceps muscles or GM with a largest mean muscle activity recorded in the GN.

The results of the simulation in the squat position agree with the findings of Isear et al (6) who studied lower limb muscle recruitment patterns of the squat using EMG. This study similarly found the largest muscle activity of the quadriceps followed by sizable activities of the muscles of the hamstrings, GM and GN.

Support for the results of the simulation in the knee flexed standing position is provided by a study performed by Escamilla (110). This study examined the muscle activity using EMG during dynamics squats between 0 and 100 degrees. One possible drawback of this study is that it measured dynamic rather than the static squats of the simulation, although there is evidence that these two types of movements provide comparable muscle activities (111). The study found that as knee flexion decreased, there was generally a reduction in the muscle activity of the quadriceps, hamstrings, and the GN. These findings match the results of the simulation which show a similar decrease in the muscle activity of quadriceps (RF

and VL), hamstrings (BF) and GN as the knee flexion is reduced between the squat and knee flexed standing positions.

The muscle activities of the knee locked standing position are validated by a report by Loram et al (5) which investigated the muscle activity of human standing. This report states that in human standing the centre of mass is positioned in front of the ankle joints requiring the plantar flexors of the foot, the GN and soleus, to maintain balance. These findings are in agreement with the results of the simulation which found the GN to be the most active. Furthermore, since there is zero or very little flexion moment on the knee during knee locked standing it is reasonable to assume that there is no requirement for the leg extensor muscles (RF and VL) which was also replicated in the simulation.

The results of these three body positions without WBV show that the muscle activities recorded with the AnyBody simulation are comparable to those gathered using EMG experimentally and therefore suggests that the model has been designed correctly at this configuration. In addition, these results form a basis for which the effects of WBV can be compared. The goal of the next analysis was to examine how the mean muscle activities of the body positions changed under the application of moderate frequency, low amplitude WBV (20 Hz, 1 mm), as shown in Figure 19. The simulation of WBV at this specification was shown to have very little effect on the mean muscle activities of the squatting position compared to the results without WBV. In contrast there was a significant increase in the muscle activities of the knee flexed standing position with activities much greater than the squatting position in the muscles of the RF and GM. Finally, the knee locked standing position resulted in calculated muscle activities which were so large that they exceeded those which were possible to produce in the human body model analysed.

Evidence that the small changes in neuromuscular activity shown by the squat position under this specification of WBV are realistic is provided by a study by Hazell et al (112). This study found that subjects with a 30 degree knee flexion subjected to vertical WBV of 25 Hz and 2 mm amplitude underwent a change in muscle activity with WBV of the VL of just 2% compared to without WBV. Although the parameters of this study differ somewhat from the 20 Hz and 1 mm

side-alternating WBV simulated, the results support the findings of the simulation that there should only be a small change in mean muscle activity at moderate frequencies and amplitudes in the squatting position.

The large changes in mean muscle activity recorded by the knee flexed standing position on the other hand are not supported by literature. One such study with contradictory results has been performed by Ritzmann et al (72) and measured EMG activity of muscles in body positions with knee flexion of 30 and 60 degrees during the application of WBV. This study found that **reducing** the knee flexion from 60 to 30 degrees resulted in decreased EMG activity of the leg extensor muscles analysed (RF, vastus medialis, tibialis anterior). These results contrast with the results of the simulation which found that the **reduced** knee flexion of the knee flexed standing position compared to the squat position showed comparable muscle activity in the knee extensor muscles (greater muscle activity in the RF but less muscle activity in the VL). The reason for the higher than expected activity of the knee extensor muscles of the knee flexed standing position under WBV is most likely due to the way WBV was modelled as discussed later in the report.

There is some evidence that supports the higher muscles activities recorded by the knee locked standing compared to flexed knee standing although not to the extent recorded. A study by Ma et al (2) compared the effects of lower limb normal and knee locked postures on muscle activity under vertical WBV. Data was collected using motion capture data used in an AnyBody model and verified by sEMG data. The muscles of the quadriceps were analysed and found to all increase in muscle activity in the knee locked position compared to the knee normal position. Even with this consideration however it is not expected that there should have been such a large increase in muscle activation with WBV compared to without WBV from this position. The reason for this error is most likely due to the way WBV was simulated in the model as discussed later.

Subsequent to discovering that the squat position was the only body position simulated which gave mean muscle activities comparable to the literature, the next stage was to analyse what the effect of simulating SCI had on this position. The results of Figure 20 showed an increase in mean muscle activity when simulating

SCI as opposed to no SCI which was justified by requirement for increased recruitment of muscle fibres at lower muscle mass. There was however a number of differences between healthy individuals and individuals with SCI, identified in the literature, which were not considered in the model. An example of this is research which has indicated that the tonic vibration reflex, responsible for muscle contractions due to vibration, often has a much more sudden onset and much higher amplitude in individuals with SCI than those in healthy subjects. The reason for this is thought to be due to excess excitability of the segmental structures in these subjects (113).

Evidence that WBV can be used to elicit muscle activity in individuals with chronic SCI has been studied by Alizadeh-Megharazi et al (114). This study found that the amplitude of vibration had the greatest influence on muscle activation, while the frequency had a lesser but still statistical significant effect on lower extremity muscle activity. A similar result was found by Craven (60) who found that neuromuscular activity of the tibialis anterior, medial gastrocnemius, and vastus lateralis increased with both frequency and amplitude of vibration. A caveat to this finding however was that increases were smaller for the motor complete SCI participants compared to the patients with motor incomplete SCI which has not been considered in this simulation.

At this stage of the investigation, the only platform type investigated had been the side-alternating platform. The next stage was to compare the effects of vertical and side-alternating WBV on the mean muscle activation. The effect of vibration type at a frequency of 30 Hz and amplitude of 2 mm, shown in Figure 21, displayed a much greater effect of vertical WBV than side-alternating WBV in increasing muscle mean muscle activity compared to without WBV in all muscles except the RF.

These results contrast those found in the literature. An example of such a study conducted by Ritzmann et al (72) similarly examined the effects of WBV applied at 30 Hz and 2 mm by vertical and side-alternating means on muscle activity in healthy individuals. These results showed a significant increase in the EMG activity in all recorded muscles for side-alternating vibration compared to vertical. This included a 91% increase in a plantar flexor muscle (gastrocnemius medialis) and a 74% increase

in a muscle of the thigh extensors (BF). In contrast to these results, the simulation found that the plantar flexor muscle (GN) and thigh extensor muscle (BF) mean activity was small in side-alternating compared to vertical WBV. The reason for this discrepancy is thought to be issues in the way vertical WBV was modelled in the simulation as discussed later in the report.

The final configuration in which muscle activities were measured was under changing WBV frequencies and amplitudes, as seen for each muscle in Figures 22-26. The overall findings were that the different muscles displayed unique trends of mean muscle activities under the same increments of frequency and amplitude. The RF (Figure 22) and VL (Figure 23) showed that all three frequencies tested had a positive influence on the mean muscle activity, especially at higher amplitudes. The BF (Figure 24) showed no effect of frequency and a negative effect of amplitude on muscle activity up until a frequency of 30 Hz where this pattern was reversed. The GM (Figure 25) showed no effect of frequency at lower amplitudes (1 mm) but did display an effect of frequency at amplitudes of 2 mm and above. Finally the GN (Figure 26) showed a maximum muscle activity at the lowest frequency tested (10 Hz) and also showed a positive effect of amplitude at this frequency. Further increases of frequency (20 Hz and 30 Hz) correlated with a reduction in the mean muscle activity recorded for this muscle.

A study concerning the effect of increasing frequencies of WBV on muscle activation has been undertaken by Pollock et al (115) on 12 healthy adults. This study produced results of the effects of different frequencies (5-30 Hz) and amplitudes (2.5-5.0 mm) of side-alternating WBV on the muscle activation of healthy volunteers. The results of this study agree with those of the simulation that the effect of frequency on muscle activation is greatest at higher amplitudes. This study also found a statistically significant difference in muscle activities of the RF between the frequencies of 5 and 30 Hz which supports the results of the simulation. This study did not however find an effect of frequency on muscle activity of the BF which contradicts the results of the simulation nor did it find an effect of frequency on the muscle activity of the GM which was found at 30 Hz in the simulation. The main reason considered for this discrepancy in results is the different body positions

analysed since the study was performed with subjects in 4.8° knee flexion as opposed to 50° in the simulation.

Further work performed by Cardinal et al (116) measured the muscle activation under increasing frequencies of WBV compared to without WBV. The EMG activity of the VL muscle was measured while the subjects experienced vertical vibration of 30-50 Hz and 10 mm amplitude. The study found a statistically significant increase in EMG activity of the VL muscle in all WBV treatment frequencies as compared to the no-vibration condition which is replicated in the simulation at 30 Hz. An interesting finding of this study is that the EMG maximum activity was found at 30 Hz with a reduction in EMG at increasing increments of frequencies. This result was not replicated in the simulation since the maximum frequency for side-alternating WBV is lower than that of vertical WBV and as such frequencies above 30 Hz were not investigated.

6.1.2 Relevance of findings

The AnyBody model successfully analysed three body positions without WBV and achieved comparable results of muscle activity as compared to literature. These results provide a useful indicator of what muscles will be active during WBV. By further modifying these body models they can be used to analyse the muscle activities for a wider range of body positions which the patient may be placed in to target regions of bone loss.

Unfortunately flaws in the model meant that it was not possible to gather as much information about the selected muscle activities with the application of WBV. In this case only the squatting position and the side-alternating WBV platform were considered to give realistic results as compared to the literature. Despite these limitations, it was possible to gather data for a variety of frequencies and amplitudes of WBV at these parameters to see what effect this had on the chosen muscles. The muscles of the RF, VL, and GM were all found to show large increases in muscle activity with increasing frequency and amplitude (more than doubling in activity at the highest frequency and amplitude specification) showing the effectiveness of WBV at stimulating these muscles in the squat position. The BF showed mixed results and the GN negative results after 10 Hz frequency indicating that the squat

position tested may not be the best way to stimulate these muscles. This information could be used to help WBV rehabilitation protocols by selecting the appropriate WBV parameters to activate certain muscles and hence target specific bone regions. Although an analysis of muscle activities is useful to gauge the activity of the muscles under a range of WBV parameters, a more useful measurand to understand the extent of the loading on the bones is to examine the muscle forces produced. This formed the second part of this investigation.

6.2 Muscle forces

In this section the muscle forces under a range of WBV parameters were determined. This was performed in order to further validate the accuracy of the model compared to studies in the literature and also to determine whether there were similar trends in muscle forces as with muscle activity as expected. The second aim was to use the values of muscle forces measured to make inferences about the loads which may be placed on different bones as a result, through knowledge of the muscle origin and insertion points on the bone.

6.2.1 Comparison with experimental results

The results of mean muscle forces without WBV, shown in Figure 27, illustrate that the greatest mean muscle force is exhibited at the VL with sizable forces also exhibited by the RF, GM, and BF. With the application of the highest specification of WBV (25 Hz, 3.5 mm), large increases in mean muscle forces were recorded in the VL, RF, GM, but not the BF or GN. A subsequent analysis of the peak muscle forces at the same specification of WBV found that these were much larger than the mean muscle forces measured. In addition, the BF which showed virtually no increase in mean muscle force with increasing frequency and amplitude of WBV, displayed a large increase in peak muscle force.

These results of mean muscle forces without WBV agree with a study by Dahlkvist et al (117) which calculated muscle forces developed during squatting and rising from a deep squat. This study found that the muscles of the quadriceps created the largest force. This is mirrored in the results of the simulation without WBV which shows the maximum mean muscle forces at the quadriceps muscles (RF and VL). In

addition the study found that the GN created a muscle force less than the quadriceps and hamstring muscles which is also replicated in the simulation.

There were no studies found of muscle forces measured during WBV to compare to the other results gathered. The absence of these figures may be due to the difficulty incurred in gathering this data in a practical setting since it cannot be directly measured non-invasively. Since the muscle forces will be expected to increase with increased muscle activity, and the muscle activity in this WBV configuration has already been validated with the literature, it is reasonable to assume the values of muscle forces measured were realistic.

6.2.2 Relevance of findings

Based on the calculation of mean muscle forces only three muscles were found to show at least a doubling in muscle forces as a result of the maximum specification of WBV (25 Hz, 3.5 mm). These muscles were the RF, VL, and GM. The forces produced by these muscles will be transferred to the origin and insertion points on the bone (Table 3). The amount of force applied to each of these points will be equal as based on the principles Newton's third law (118) that every action should have an equal and opposite reaction. The origin and insertion points of these muscles show that the mean forces will be expected to act on the anterior inferior ilium, proximal end of the tibia, proximal end of the femur, sacrum, and coccyx.

It has already been discussed earlier in the report that forces are required to activate mechanotransduction and ensure a healthy bone mass. In addition, Harold Frost's mechanostat theory was discussed which stated that bone remodelling is driven by the maximum forces the bone is exposed to. Based on this evidence it is reasonable to assume that it is the peak, rather than the mean forces measured which are of most interest in this investigation.

Analysing the peak muscle forces, shown in Figure 28, the previously stated three muscles also show at least a doubling in peak muscle forces at the maximum WBV specification (25 Hz, 3.5 mm). In addition to this, the BF also shows a greater than doubling of peak muscle forces. With consideration of the origin and insertion points for all these muscles considered there would be expected to be a large increase in the

peak forces at the anterior inferior ilium, proximal end tibia, proximal end and shaft of the femur, proximal end of the fibula, sacrum, coccyx, and ischium.

6.3 Limitations and improvements to the investigation

During the course of the discussion section it has been mentioned that limitations of the way WBV was simulated may have caused erroneous results, as in the case of unusually high muscle activity for two of the body positions under WBV and the case of vertical WBV for the squatting position. By fixing these issues it would be possible to determine more information of variations of muscle behaviour under different body positions and vibration types. This would better enable specific vibration parameters to be tailored to the individual with SCI to target previously measured areas of bone loss. In this section the current limitations will be discussed and possible ways to improve on them in subsequent models suggested.

One aspect of the model which could be considered a limitation of the model is the design of how the body connects to the WBV platform. In this simulation it was designed so that the feet of the model were connected to the platform with drivers. If this were truly the case in real life, the feet of the subject would be completely fixed to the platform. This is obviously not the case since the subject's feet would be expected to leave the platform when the platform is accelerating downwards. It is thought that modelling the human body in this way may subject the body to unrealistically high changes in accelerations resulting in increased muscle activity. One way the issue of the foot not being in constant contact with an object has been dealt with in previous studies is through the use of "conditional contact". This method uses muscles between the object and the human body which are only active under certain conditions and therefore ground reaction forces are only conditionally generated. Although attempts were made to implement this in this model, the complexity was too great to accurately implement in the time frame for this project.

Another limitation of the model is the static nature of the body positions. Body positions which were intended to be fixed such as the feet on the platform were defined with "hard" drivers. The remaining constraints such as the joints of the body were defined with "soft" drivers with a weight function. This weight function defines how much emphasis is placed on some constraints with respect to others. Without

detailed analysis of motion capture data during WBV it is challenging to know exactly what weight functions to assign to these joints, and by default AnyBody automatically assigns each joint an equal one. Additionally the body position models fail to consider any adjustment the subjects may make while on the WBV platform for the sake of comfort. A way that this could be rectified is by using motion capture data of an individual with SCI while undergoing WBV rather than attempting to replicate the movement using approximations. The obvious drawback of this method is that it would be time consuming to take motion capture data and also require the use of expensive WBV equipment.

A final limitation of the analysis is that the peak forces produced by the muscle were assumed to act on approximate regions of the bone identified by the origin and insertion points of the muscle. This only gives a rough estimation of how the forces on the muscle act on the bone. An example of a study which has used more complex modelling between the muscle forces and bone has been performed by Bitsakos et al (119). This study measured the strain adaptive remodelling produced on different areas of the bone as a result of increasingly complex muscle force configurations. If a similar finite element model could be combined with the results of the simulation, it would allow much more detailed information of location and magnitude of the resulting bone loading.

6.4 Future work

6.4.1 Validation of the model

Due to limitations in data available it was not possible to perform validation of this model. One of the ways in which AnyBody models of muscle activation have been validated in the past is by comparing the muscle activations computed with EMG muscle activities of the subject such as the study by Ma et al (2). This method of validation was not possible for this investigation since motion capture data was not used and therefore a direct comparison of data could not be made with the EMG of an individual.

One method of validations which is feasible for this analysis is to validate the accelerations of the body parts determined during the simulation to ensure these are

realistic. These accelerations could be compared with a number of studies which have used motion capture to determine the relative movement of markers at certain bony landmarks. An example of data which could be used to verify the results are the published accelerations of the marker positions of the body under side-alternating vibration performed by Harris (120). This is shown in Figure 30 where the y-axis represents RMS acceleration (g).

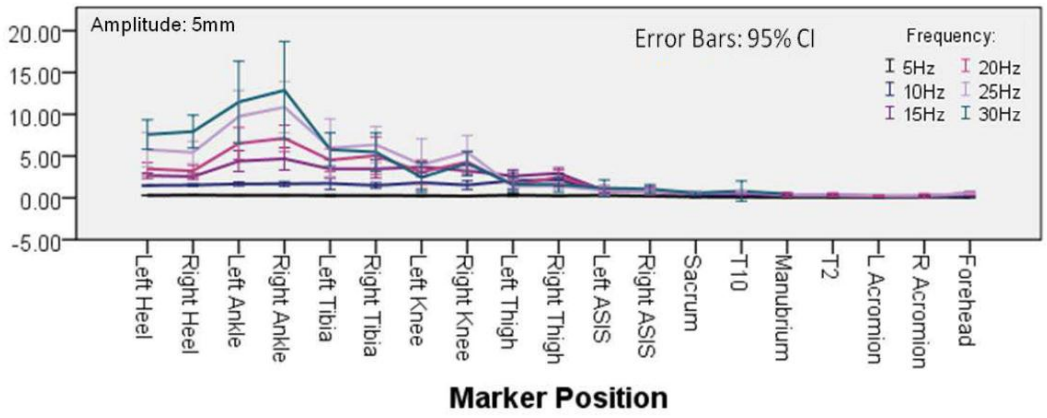

Figure 30: RMS accelerations delivered by the Galileo 900 platform at frequencies between 5 and 30 Hz and amplitudes between 0 mm and 5 mm, taken from Harris (120)

6.4.2 Further simulations

During the course of this investigation a number of parameters of WBV which could be useful in the design of intervention protocols in individuals with SCI were analysed. A parameter which was not explored due to time constraints was the simulation of an individual with assistive adaptations (such as used to assist passive standing or place the individual in a supine tilt). These interventions are required in most individuals with SCI to undergo WBV since they are unable to stand on a vibration plate unassisted (56).

Only one relevant paper studied the effects of assistive adaptations on the muscle activity under WBV. This study, performed by Herrero et al (57), tested the muscle activities produced by individuals with motor complete SCI undergoing side-alternating vibration while on a tilt table. This study measured an increase in the EMG activity of the VL and vastus medialis but found that this increase was independent of the applied frequency.

Further work into the type of squat was not performed in this investigation but work in the literature provides some indication of values which could be expected. For instance, a study by Roelants et al (121) examined the effect of different types of squats on muscle activity under vertical WBV (35 Hz, 2.5 mm amplitude). The positions studied were the high squat, low squat, and 1-legged squat. This study used EMG analysis to determine the muscle activity of the RF, VL, vastus medialis, and GN muscles of the dominant leg. In this study the vibration effect of the high squat was not found to be significantly different from the low squat. This study did however find a significant increase in activity in all muscles and exercises compared to the non-vibrating conditions as found in this simulation.

Chapter 7: Conclusions

The results of muscle activity in various body positions without the application of WBV gave realistic muscle activities which correlated well with findings from EMG in the literature. Unfortunately subsequent analyses with the application of WBV showed unrealistic muscle activities in the body positions of the knee flexed and knee locked standing positions and with the vertical WBV platform type. The reasons for these results were thought to be due to the way the feet were modelled to be connected to the platform as well as inaccuracies in the body movement during WBV. Other limitations of the model included the way in which the SCI injury was simulated in the model which accounted for the loss in muscle mass but not for an increased vibration reflex in SCI sufferers or the difference in response for individuals with either motor incomplete and complete SCI.

The model did however show success in gathering both accurate mean muscle activities and muscle forces as compared to the literature in the squatting position under side-alternating WBV. This simulation enabled data to be gathered on specific muscles under different frequencies and amplitudes which demonstrate the potential of this kind of simulation to inform rehabilitation intervention design. One of the drawbacks of the use of the simulation is that it can only provide estimations of regions of bone loading based on the origin and insertion points of the muscle on the bone. It is the opinion of the author that this could be improved by implementing finite element analysis of the bones using the forces provided by the muscles to achieve more accurate results of the loading of the bones.

Improvements to the model which allow analysis of the human model under different body positions and vibration types will expand the potential of the simulation as a method of informing rehabilitation intervention design. In addition a validation of the accelerations generated in the human body during the simulation is required to ensure the accelerations generated are realistic before this simulation can be applied clinically. Finally, further simulations which incorporate the assistive devices commonly used applying WBV to individuals with SCI such as tilt plate or standing

frame would be expected to increase the accuracy of calculations of muscle behaviour for this purpose.

Chapter 8: Bibliography

1. Davis R, Sanborn C, Nichols D, et al. The effects of whole body vibration on bone mineral density for a person with a spinal cord injury: a case study. Adapt Phys Activ Q. 2010; 27(1).

2. Ma C, Zhang M, Tan C, et al. Analysis of Lower-limb Muscle Activities During Whole body Vibration with Different Standing Postures. 3rd International Conference on Biomedical Engineering and Informatics. 2010.

3. Jenkins BD. Hollinshead's Functional Anatomy of the Limbs and Back: Saunders; 2002.

4. Bones of the Lower Extremeties. Skeletal System Diagrams & Links. [Online]. [cited 2015 August 5. Available from: https://jb004.k12.sd.us/my%20website%20info/human%20anatomy/SKELETAL%20SYSTEM/SKELETAL%20SYSTEM%20DIAGRAMS.htm.

5. Loram ID, Maganaris CN, Lakie M. Paradoxical muscle movement in human standing. J Physiol. 2004; 556(3).

6. Isear JA, Erickson JC, Worrell TW. EMG analysis of lower extremity muscle recruitment patterns during an unloaded squat. Med Sci Sports Exerc. 1997; 29(4).

7. Rucci N. Molecular biology of bone remodelling. Clin Cases Miner Bone Metab. 2008; 5(1).

8. Shabestari M, Eriksen EF. Mechanisms of Bone Remodeling. In W SD. Osteoporosis: Diagnosis and Management.: John Wiley & Sons; 2013.

9. Jiang SD, Dai LY, Jiang LS. Osteoporosis after spinal cord injury. Osteoporosis Int. 2006; 17(2).

10. Bonjour JP, Ammann P, Rizzoli R. Importance of preclinical studies in the development of drugs for treatment of osteoporosis: a review related to the 1998 WHO guidelines. Osteoporosis Int. 1999; 9(5).

11. Guidelines for preclinical evaluation and clinical trials in osteoporosis: World Health Organisation; 1998.

12. Bone Health and Osteoporosis: A Report of the Surgeon General. US Department of Health and Human Services. 2004.

13. R N. Everything you need to know about osteoporosis: Sheldon Press; 1990.

14. Rahimi-Movaghar V, Sayyah MK, Akbari H, et al. Epidemiology of Traumatic Spinal Cord Injury in Developing Countries: A Systematic Review. Neuroepidemiology. 2013; 41(2).

15. Preserving and Developing the National Spinal Cord Injury Service. British Association of Spinal Cord Injury Specialists; 2009.

16. Facts and Figures. Spinal Research. [Online]. [cited 2015 July 9. Available from: http://www.spinal-research.org/research-matters/spinal-cord-injury/facts-and-figures/.

17. National Spinal Cord Injury Statistical Centre. [Online].; 2014 [cited 2015 July 15. Available from: https://www.nscisc.uab.edu/PublicDocuments/reports/pdf/2014%20NSCISC%20Annual%20Statistical%20Report%20Complete%20Public%20Version.pdf.

18. Thompson C, Mutch J, Parent S, et al. The changing demographics of traumatic spinal cord injury: An 11-year study of 831 patients. J Spinal Cord Med. 2015; 38(2).

19. Miele VJ, Panjabi MM, Benzel EC. Anatomy and biomechancs of the spinal column and cord. In Handbook of Clinical Neurology.: J Clin Pathol; 2012.

20. Spinal Cord. UC San Diego Health. [Online]. [cited 2015 14 July. Available from: http://health.ucsd.edu/specialties/neuro/specialty-programs/paralysis-center/PublishingImages/spinal%20cord%203.jpg.

21. Kirshblum SC, Burns SP, Biering-Sorensen F, et al. International standards for neurological classification of spinal cord injury (Revised 2011). J Spinal Cord Med. 2011; 34(6).

22. Burns A, Marino RJ, Flanders AE, et al. Clinical diagnosis and prognosis following spinal cord injury. In Handbook of Clinical Neurology.; 2012.

23. McKinley WO, Jackson AB, Cardenas DD, et al. Long-Term Medical Complications After Traumatic Spinal Cord Injury: A Regional Model Systems Analysis. Arch Phys Med Rehabil. 1999; 80(11).

24. McKinley WO, Gittler MS, Kirshblum SC, et al. Medical complications after spinal cord injury: Identification and management. Arch of Phys Med and Rehab. 2002; 83(1).

25. Sezer N, Akkus S, Ugurlu FG. Chronic complications of spinal cord injury. World J Orthop. 2015; 6(1).

26. Giangregorio L, McCartney N. Bone Loss and Muscle Atrophy in Spinal Cord Injury: Epidemiology, Fracture Prediction, and Rehabilitation Strategies. J Spinal Cord Med. 2006; 29(5).

27. Sedlock DA, Laventure SJ. Body composition and resting energy expenditure in long term spinal cord injury. Paraplegia. 1990; 28(7).

28. Wilmet E, Ismail AA, Heilporn A, et al. Longitudinal study of the bone mineral content and of soft tissue composition after spinal cord section. Paraplegia. 1995; 33(11).

29. Modlesky CM, Bickel CS, Slade JM, et al. Assessment of skeletal muscle mass in men with spinal cord injury using dual-energy X-ray absorptiometry

and magnetic resonance imaging. J Appl Physiol. 2004; 96(2).

30. Chantraine A, Nusgens B, Lapiere CM. Bone remodelling during the development of osteoporosis in paraplegia. Calcif Tissue Int. 1986; 38(6).

31. Totosy de Zepetnek JO, Giangregorio LM, Craven C. Whole-body vibration as potential intervention for people with low bone mineral density and osteoporosis: A review. J Rehabil Res Dev. 2009; 46(4).

32. Dauty M, Perrouin Verbe B, Maugars Y, et al. Supralesional and sublesional bone mineral density in spinal cord-injured patients. Bone. 2000; 27(2).

33. Vico L, Collet P, Guignandon A, et al. Effects of long-term microgravity exposure on cancellous and cortical weight-bearing bones of cosmonauts. Lancet. 2000; 355(9215).

34. Chantraine A, Ouwenaller CV, Hachen HJ, et al. Intra-medullary pressure and intra-osseous phlebography in paraplegia. Paraplegia. 1979; 17.

35. Maimoun L, Lumbroso S, Paris F, et al. The role of androgens or growth factors in the bone resorption process in recent spinal cord injured patients: a cross-sectional study. Spinal Cord. 2006; 44(12).

36. Jiang SD, Jiang LS, Y DL. Effects of spinal cord injury on osteoblastogenesis, osteoclastogenesis and gene expression profiling in osteoblasts in young rats. Osteoporos Int. 2007; 18(3).

37. Freeman LW. The Metabolism of Calcium in Patients with Spinal Cord Injuries. Ann Surg. 1949; 129(2).

38. Schneider VS, McDonald J. Skeletal calcium homeostasis and countermeasures to prevent disuse osteoporosis. Calcif Tissue Int. 1984; 36(1).

39. Hulley SB, Vogel JM, Donaldson CL, et al. The effects of supplemental oral phosphate on the bone mineral changes during prolonged bed rest. J Clin

Invest. 1971; 50(12).

40. Maimoun L, Fattal C, Micallef JP, et al. Bone loss in spinal cord-injured patients: from physiopathology to therapy. Spinal Cord. 2006; 44(4).

41. Body JJ. Calcitonin for the long-term prevention and treatment of postmenopausal osteoporosis. Bone. 2002; 30(5).

42. Braddom RL, Erickson R, Johnson EW. Ineffectiveness of calcitonin on osteoporosis in paraplegic rats. Arch Phys Med Rehabil. 1973; 54(4).

43. Moran de Brito CM, Battistella LR, Saito ET, et al. Effect of alendronate on bone mineral density in spinal cord injury patients: a pilot study. Spinal Cord. 2005; 43(6).

44. Nance PW, Schryvers O, Leslie W, et al. Intravenous pamidronate attenuates bone density loss after acute spinal cord injury. Arch Phys Med Rehabil. 1999; 80(3).

45. Leblanc AD, Schneider VS, Evans HJ, et al. Bone minearal loss and recovery after 17 weeks of bed rest. J Bone Miner Res. 1990; 5(8).

46. Jones LM, Legge M, Goulding A. Intensive exercise may preserve bone mass of the upper limbs in spinal cord injured males but does not retard demineriliśation of the lower body. Spinal Cord. 2002; 40(5).

47. Frotzler A, Coupaud S, Perret C, et al. High-volume FES-cycling partially reverses bone loss in people with chronic spinal cord injury. Bone. 2008; 43(1).

48. Angle SR, Sena K, Sumner DR, et al. Osteogenic differentiation of rat bone marrow stomal cells by various intensities of low-intensity pulsed ultrasound. Ultrasonics. 2011; 51(3).

49. Lim D, Ko CY, Seo DH, et al. Low-intensity ultrasound stimulation prevents osteoporotic bone loss in young adult ovariectomized mice. J Orthop Res.

2011; 29(1).

50. Warden SJ, Bennell KL, Matthews B, et al. Efficacy of Low-intensity Pulsed Ultrasound in the Prevention of Osteoporosis Following Spinal Cord Injury. Bone. 2001; 29(5).

51. Sanders CE. Cardiovascular and Peripheral Vascular Diseases: Treatment by a Motorised Oscillating Bed. JAMA. 1936; 106(11).

52. Rittweger J. Vibration as an exercise modality- how it may work, and what its potential might be. Eur J Appl Physiol. 2010; 108(5): p. 877-904.

53. The physical principles of sound. JISC Digital Media. [Online]. [cited 2015 July 14. Available from: http://www.jiscdigitalmedia.ac.uk/guide/the-physical-principles-of-sound.

54. Cardinale M, Wakeling J. Whole body vibration exercise: are vibrations good for you? Br J Sports Med. 2005; 39(9).

55. Rauch F, Sievanen H, Boonen S, et al. Reporting whole-body vibration intervention studies: Recommendations of the International Society of Musculoskeletal and Neuronal Interactions. J Musculoskelet Neuronal Interact. 2010; 10(3).

56. Asselin P, Spungen AM, Muir JW, et al. Transmission of low-intensity vibration through the axial skeleton of persons with spinal cord injury as a potential intervention for preservation of bone quantity and quality. J Spinal Cord Med. 2011; 34(1).

57. Herrero AJ, Menendez H, Gil L, et al. Effects of whole-body vibration on blood flow and neuromuscular activity in spinal cord injury. Spinal Cord. 2011; 49(4).

58. Sayenko DG, Masani K, Alizadeh-Meghrazi M, et al. Acute effects of whole body vibration during passive standing on soleus H-reflex in subjects with and

without spinal cord injury. Neurosci Lett. 2010; 482(1).

59. Alizadeh-Meghrazi M, Masani K, Popovic MR. Whole-body vibration during passive standing in individuals with spinal cord injury: effects of plate choice, frequency, amplitude, and subject's posture on vibration propagation. PM&R. 2012; 4(12).

60. Craven CTD. Development and Evaluation of Rehabilitation Technologies for Early-Stage Spinal Cord Injury. University of Glasgow. 2014.

61. Ness LL, Field-Fote EC. Whole-body vibration improves walking function in individuals with spinal cord injury: a pilot study. Gait Posture. 2009; 30(4).

62. Cormie P, Deane RS, Triplett T, et al. Acute effects of whole-body vibration on muscle activity, strength, and power. J Strength Cond Res. 2006; 20(2).

63. Fethke NB. Application of surface electromyography in assessing occupational exposure to forceful exertion. The University of Iowa. 2006.

64. Merlo A, Campanini I. Technical Aspects of Surface Electromyography for Clinicians. The Open Rehabilitation Journal. 2010; 3.

65. Prisby RD, Lafage-Proust MH, Malaval L, et al. Effects of whole body vibration on the skeleton and other organ systems in man and animal models: what we know and what we need to know. Ageing Res Rev. 2008; 7(4).

66. Hsieh YF, Turner CH. Effects of loading frequency on mechanically induced bone formation. J Bone Miner Res. 2001; 16(5).

67. Schoenau E, Fricke O. Mechanical influences on bone development in children. Eur J Endocrinol. 2008; 159(1).

68. Gail PD, Lance JW, Neilson PD. Differential effects on tonic and phasic reflex mechanisms produced by vibration of muscles in man. J Neurol Neurosurg Psychiatry. 1966; 29(1).

69. Zhou Z, Zheng L, Wei D, et al. Muscular strength measurements indicate bone mineral density loss in postmenopausal women. Clin Interv Aging. 2013; 8.

70. Turner CH. Three rules for bone adaptation to mechanical stimuli. Bone. 1998; 23(5).

71. Rubin CT, Lanyon LE. Regulation of bone formation by applied dynamic loads. J Bone Joint Surg Am. 1984; 66(3).

72. Ritzmann R, Gollhofer A, Kramer A. The influence on vibration type, frequency, body position and additional load on the neuromuscular activity during whole body vibration. Eur J Appl Physiol. 2013; 113(1): p. 1-11.

73. Pel JJM, Bagheri J, M VDL, et al. Platform accelerations of three different whole-body vibration devices and the transmission of vertical vibrations of the lower limbs. Medical Engineering & Physics. 2009; 31: p. 937-944.

74. Corrie H, Brooke-Wavell K, Mansfield N, et al. Effect of whole body vibration on bone formation and resorption in older patients: A randomised controlled trial. Osteoporosis Int. 2007; 18.

75. Rubin C, Pope M, Fritton JC, et al. Transmissibility of 15-hertz to 35-hertz vibrations to the human hip and lumbar spine: determining the physiologic feasibility of delivering low-level anabolic mechanical stimuli to skeletal regions at greatest risk of fracture because of osteoporosis. Spine. 2003; 28(23).

76. Pasqualini M, Lavet C, Elbadaoui M, et al. Skeletal site-specific effects of whole body vibration in mature rats: from deleterious to beneficial frequency-dependent effects. Bone. 2013; 55(1).

77. Pitukcheewanont P, Safani D. Extremely low-level, short-term mechanical stimulation increases cancellous and cortical bone density and muscle mass of children with low bone density: a pilot study. Endocrinologist. 2006; 16(3).

78. Rubin C, Recker R, Cullen D, et al. Prevention of Postmenopausal Bone Loss by a Low-Magnitude, High-Frequency Mechanical Stimuli: A Clinical Trial Assessing Compliance, Efficacy, and Safety. J Bone Miner Res. 2004; 19(3).

79. Verschueren SM, Roelants M, Delecluse C, et al. Effect of 6-Month Whole Body Vibration Training on Hip Density, Muscle Strength, and Postural Control in Postmenopausal Women: A Randomized Controlled Pilot Study. Journal of Bone and Mineral Research. 2003; 19(3): p. 352-9.

80. Torvinen S, Kannus P, Sievanen H, et al. Effect of 8-Month Vertical Whole Body Vibration on Bone, Muscle Performance, and Body Balance: A Radomized Controlled Study. J Bone Miner Res. 2003; 18(5).

81. Gusi N, Raimundo A, Leal A. Low-frequency vibratory exercise reduces the risk of bone fracture more than walking: a randomized controlled trial. BMC Musculoskeletal Disord. 2006; 7(92).

82. Heidari B, Hosseini R, Javadian Y, et al. Factors affecting bone mineral density in postmenopausal women. Arch Osteoporos. 2015; 10(1).

83. Santin-Medeiros F, Santos-Lozano A, Rey-Lopez JP, et al. Effects of eight months of whole body vibration training on hip bone mass in older women. Nutr Hosp. 2015; 31(4).

84. Liphardt AM, Schipilow J, Hanley DA, et al. Bone quality in osteopenic postmenopausal women is not improved after 12 months of whole-body vibration training. Osteoporos Int. 2015; 26(3).

85. LeBlanc AD, Spector ER, Evans HJ, et al. Skeletal responses to space flight and the bed rest analog: A review. J Musculoskelet Neuronal Interact. 2007; 7(1): p. 33-47.

86. Goodship AE, Cunningham JL, Oganov V, et al. Bone loss during long term space flight is prevented by the application of a short term impulsive

mechanical stimulus. Acta Astronautica. 1998; 45(1): p. 65-75.

87. Muir J, Xia Y, Holguin N, et al. Retention of bone density and postural status with a non-invasive extremely low level mechanical signal: a ground based evaluation of efficacy. Bioengineering Conference. 2007.

88. Bramlett HM, Dietrich WD, Marcillo A, et al. Effects of low intensity vibration on bone and muscle in rats with spinal cord injury. Osteoporosis Int. 2014; 25(9).

89. Brooke-Wavell K, Mansfield NJ. Risks and benefits of whole body vibration training in older people. Age and Ageing. 2009; 38.

90. Kiiski J, Heinonen A, Jarvinen TI, et al. Transmission of Vertical Whole Body Vibration to the Human Body. J Bone Miner Res. 2008; 23(8).

91. Randall JM, T MR, Stiles JA. Resonant frequencies of standing humans. Ergonomics. 1997; 40(9).

92. Abercromby AFJ, Amonette WE, Layne CS, et al. Vibration Exposure and Biodynamic Responses during Whole-Body Vibration Training. Med Sci Sports Exerc. 2007; 39(10).

93. Company. AnyBody Technology. [Online]. [cited 2015 August 4. Available from: http://www.anybodytech.com/?id=186.

94. Damsgaard M, Rasmussen J, Christensen ST, et al. Analysis of musculoskeletal systems in the AnyBody Modelling System. Simulation Modelling Practice and Theory. 2006; 14(8): p. 1100-1111.

95. Publications. AnyBody Technology. [Online]. [cited 2015 July 14. Available from: http://www.anybodytech.com/index.php?id=publications.

96. Getting Started: The Model Repository (AMMR). AnyBody Technology. [Online]. [cited 2015 July 14. Available from: http://www.anybodytech.com/fileadmin/AnyBody/Docs/Tutorials/A_Getting_

started_AMMR/intro.html.

97. The Body Models. AnyBody Technology. [Online]. [cited 2015 July 14. Available from: http://www.anybodytech.com/fileadmin/AnyBody/Docs/Tutorials/A_Getting_started_AMMR/lesson2.html.

98. Joint to Joint Scaling Methods. AnyBody Technology. [Online]. [cited 2015 July 14. Available from: http://www.anybodytech.com/fileadmin/AnyBody/Docs/Tutorials/chap10_Scaling/lesson1.html.

99. Inverse Dynamics of Muscle Systems. AnyBody Technology. [Online]. [cited 2015 August 3. Available from: http://www.anybodytech.com/fileadmin/AnyBody/Docs/Tutorials/chapX_MuscleRecruitment/Inverse_dynamics.html.

100. AnyBody Technology web cast: Gait Modelling. AnyBody Technology. [Online]. [cited 2015 July 29. Available from: http://www.anybodytech.com/fileadmin/examples/Q_and_A_Gait_webcast.htm.

101. Zee M, Dalstra M, Cattaneo PM, et al. Validation of a musculo-skeletal model of the mandible and its application to mandibular distraction osteogenesis. Journal of Biomechanics. 2007; 40.

102. Salkind JN. Statistics for People Who Hate Statistics: Sage; 2011.

103. Li W, Zhang M, Lv G, et al. Biomechanical response of the musculoskeletal system to whole body vibration using a seated driver model. International Journal of Industrial Ergonomics. 2015; 45: p. 91-97.

104. About us.Galileo training. [Online]. [cited 2015 July 15. Available from: http://www.galileo-training.com/de-english/about-us.html.

105. About. Power Plate. [Online]. [cited 4 August 2015. Available from: https://powerplate.com/about-power-plate.

106. Lesson 2: Scaling based on external body measurements. AnyBody Technology. [Online]. [cited 2015 August 2. Available from: http://www.anybodytech.com/fileadmin/AnyBody/Docs/Tutorials/chap10_Scaling/lesson2.html.

107. Hwang S, Kim Y, Kim Y. Lower extremity joint kinetics and lumbar curvature during squat and stoop lifting. BMC Musculoskeletal Dis. 2009; 10(15).

108. Rasmussen J, Kiis A. AnyBody Technology. [Online]. [cited 2015 July 30. Available from: http://www.anybodytech.com/fileadmin/examples/ScalingWebcast.pdf.

109. Schubert H. Galileo for Rehabilitation and Therapy. Novotec Medical. [Online].; 2015.

110. Escamilla RF. Knee biomechanics of the dynamic squat exercise. Med Sci Sports Exerc. 2001; 33(1).

111. Clement J, Hagenmeister N, Aissoaoui R, et al. Comparison of quasi-static and dynamic squats: A three-dimensional kinematic, kinetic and electromyographic study of the lower limbs. Gait Posture. 2014; 40(1).

112. Hazell TJ, Jakobi JM, Kenno KA. The effects of whole-body vibration on upper- and lower-body EMG during static and dynamic contractions. Appl Physiol Nutr Metab. 2007; 32(6).

113. Sherwood AM, McKay WB, Dimitrijevic MR. Motor control after spinal cord injury: assessment using surface EMG. Muscle Nerve. 1996; 19(8).

114. Alizadeh-Meghrazi M, Masani K, Zariffa J, et al. Effect of whole-body vibration on lower-limb EMG activity in subjects with and without spinal cord injury. J Spinal Cord Med. 2014; 37(5).

115. Pollock RD, Woledge RC, Mills KR, et al. Muscle activity and accerelation during whole body vibration: Effect of frequency and amplitude. Clin Biomech. 2010; 25(8).

116. Cardinale M, Lim J. Electromyography Activity of Vastus Lateralis Muscle During Whole-Body Vibrations of Different Frequencies. J Strength Cond Res. 2003; 17(3).

117. Dahlkvist NJ, Mayo P, Seedhom BB. Forces during squatting and rising from a deep squat. Eng Med. 1982; 11(2).

118. Herman PI. Physics of the Human Body: Springer; 2008.

119. Bitsakos C, Kerner J, Fisher I, et al. The effect of muscle loading on the simulation of bone remodelling in the proximal femur. Journal of Biomechanics. 2005; 38(1).

120. Harris LC. Evaluation of the Impact of Mechanical Vibration on the Adult Skeleton. University of Leeds. 2015.

121. Roelants M, Verschueren SMP, Delecluse C, et al. Whole-body-vibration-induced increase in leg muscle activity during different squat exercises. J Strength Cond Res. 2006; 20(1).

Chapter 9: Appendix

9.1 Mannequin file

This section outlines all the changes which were made to the Mannequin file of the altered AUUHuman body model.

9.1.1 Body positions

Changes to the body position of the human model to achieve the different body positions are displayed here.

9.1.1.1 Squat

```
AnyVar PelvisRotX=0;
AnyVar PelvisRotY=0;
AnyVar PelvisRotZ=-15;

AnyVar PelvisThoraxExtension=-15;
AnyVar PelvisThoraxLateralBending=0;
AnyVar PelvisThoraxRotation=0;

AnyVar HipFlexion = 15;
AnyVar HipAbduction = 5.0;
AnyVar HipExternalRotation = 0.0;

AnyVar KneeFlexion = 50;
AnyVar AnklePlantarFlexion =15.0;
AnyVar SubTalarEversion =0.0;
```

9.1.1.2 Knee flexed standing

```
AnyVar PelvisThoraxExtension=-10;
AnyVar PelvisThoraxLateralBending=0;
AnyVar PelvisThoraxRotation=0;

AnyVar HipFlexion = 10;
AnyVar HipAbduction = 5.0;
AnyVar HipExternalRotation = 0.0;

AnyVar KneeFlexion = 20;
AnyVar AnklePlantarFlexion =10;
AnyVar SubTalarEversion =0.0;
```

9.1.2 Vibration Parameters

The parameters defined in the mannequin file, which changed the parameters of WBV applied including the distance apart of the feet of the model, frequency and amplitude of vibration applied.

```
AnyFolder PlateModel =
{
AnyVar DistanceFeetApart = 0.4;
AnyVar Frequency = 20;
AnyVar Amplitude = 0.001;
AnyVar WidthPlatform = 0.65;
AnyVar CentreNodeHeight = 0.06;
AnyVar CentreNodeForward = 0;
AnyVar footpos=0;
};
```

9.2 Reference nodes defined

This section outlines the reference nodes which were defined for the final WBV model for both side-alternating and vertical vibration. These nodes were used to define the position of the feet relative to the platform.

```
AnyRefNode &HeelR =
..HumanModel.BodyModel.Right.Leg.Seg.Foot.HeelNode;
HeelR =
{
  AnyDrawNode draw =
  {
    ScaleXYZ = 0.015 * {1,1,1};
    RGB = {1,0,0};
  };
};

AnyRefNode &ToeR =
..HumanModel.BodyModel.Right.Leg.Seg.Foot.ToeJoint;
ToeR =
{
  AnyDrawNode draw =
  {
    ScaleXYZ = 0.015 * {1,1,1};
    RGB = {1,0,0};
  };
};
```

```
AnyRefNode &HeelL =
..HumanModel.BodyModel.Left.Leg.Seg.Foot.HeelNode;
HeelL =
{
  AnyDrawNode draw =
  {
    ScaleXYZ = 0.015 * {1,1,1};
    RGB = {1,0,0};
  };
};

AnyRefNode &ToeL =
..HumanModel.BodyModel.Left.Leg.Seg.Foot.ToeJoint;
ToeL =
{
  AnyDrawNode draw =
  {
    ScaleXYZ = 0.015 * {1,1,1};
    RGB = {1,0,0};
  };
};
```

9.3 Defining the vibration plate

This section displays the code used to define the location of the platform in the global (Origin) reference frame. The reference nodes “RightFootCon” and “LeftFootCon” are the nodes of the platform that the feet of the human body model were defined relative to.

```
AnyFolder Environment =
{
//*******************************************************
//  VIBRATION PLATE
//*******************************************************
  AnyFolder &PlatePara =
..HumanModel.Mannequin.PlateModel;

  AnyVar RightFoot = PlatePara.DistanceFeetApart/2;
  AnyVar LeftFoot = -RightFoot;

  AnyVar RightEdgePlat = PlatePara.WidthPlatform/2;
  AnyVar LeftEdgePlat = -RightEdgePlat;

  AnyVar CentreHeight = 0.06;
  AnyVar CentreForward = 0;
```

```
  AnyFixedRefFrame Origin =
  {
    AnySeg Plate =
    {
      Jii = {1,1,1}*0.01;
      r0 = {0.255, 0.06, 0};
      Mass = 1000;
      AnyDrawSeg drw = {};
      AnyRefNode Corner =
      {
      sRel = {-0.255,-0.06,0.325};
      ARel = RotMat (90*pi/180, y);

      AnyDrawSTL DrwPlate =
      {
        FileName = "Plate.stl";
        Opacity = 0.5;
        ScaleXYZ = {0.001, 0.001, 0.001};
        RGB = {0.5,0.5,0.5};
      };
    };

      AnyRefNode RightFootCon = {
        sRel = {...CentreForward, ...CentreHeight,
...RightFoot};
        AnyDrawNode draw ={
          ScaleXYZ = {1,1,1}*0.015;
          RGB = {0,0,1};
        };
      };
      AnyRefNode LeftFootCon = {
        sRel = {...CentreForward, ...CentreHeight,
...LeftFoot};
        AnyDrawNode draw ={
          ScaleXYZ = {1,1,1}*0.015;
          RGB = {0,0,1};
        };
      };
    };
  };
};
```

9.4 Joints and drivers

The joints and drivers defined for model. The kinematic measures are a requirement for the drivers and define one reference frame which is being driven relative to another.

9.4.1 Kinematic measures

In this case there are kinematic measures which define the linear position of the vibration plate “PlateLin” and the rotational position of the vibration plate “PlateRot”. There are also kinematic measures which define the position of reference nodes of the feet relative to a node on the vibration plate, e.g. “ToePosR”. Finally, there are kinematic measures which define the linear position of pelvis and lumbar segment relative to the global reference frame to try and simulate the movement of the body during side-alternating WBV.

```
AnyFolder KinematicMeasures =
{
  AnyKinLinear PlateLin =
  {
    AnyFixedRefFrame &Ground =
Main.Model.Environment.Origin;
    AnySeg &ref = Main.Model.Environment.Origin.Plate;
  };

  AnyKinRotational PlateRot =
  {
    Type = RotAxesAngles;
    AnyFixedRefFrame &Ground =
Main.Model.Environment.Origin;
    AnySeg &ref = Main.Model.Environment.Origin.Plate;
  };

  AnyKinLinear ToePosR = {
    AnyRefNode &Plate =
Main.Model.Environment.Origin.Plate.RightFootCon;
    AnyRefNode &Ball =
.....HumanModel.BodyModel.Right.Leg.Seg.Foot.ToeJoint;
  };

  AnyKinLinear HeelPosR = {
    AnyRefNode &Plate =
Main.Model.Environment.Origin.Plate.RightFootCon;
```

```
    AnyRefNode &target =
.....HumanModel.BodyModel.Right.Leg.Seg.Foot.HeelNode;
  };

  AnyKinLinear ToePosL = {
    AnyRefNode &Plate =
Main.Model.Environment.Origin.Plate.LeftFootCon;
    AnyRefNode &Ball =
.....HumanModel.BodyModel.Left.Leg.Seg.Foot.ToeJoint;
  };

  AnyKinLinear HeelPosL = {
    AnyRefNode &Plate =
Main.Model.Environment.Origin.Plate.LeftFootCon;
    AnyRefNode &target =
.....HumanModel.BodyModel.Left.Leg.Seg.Foot.HeelNode;
  };

  AnyKinLinear Pelvis =
  {
    AnyFixedRefFrame &Ground =
Main.Model.Environment.Origin;
    AnySeg &PelvisSeg =
Main.HumanModel.BodyModel.Trunk.SegmentsLumbar.PelvisSeg;
  };

  AnyKinLinear LumbarPos =
  {
  AnyFixedRefFrame &Ground =
Main.Model.Environment.Origin;
  AnyRefNode &ref =
Main.HumanModel.BodyModel.Trunk.SegmentsLumbar.L1Seg.
LINodeSuperior;
  };
};
```

9.4.2 Side-alternating WBV

In this section the three linear DoF are fixed, two of the rotational DoF are fixed, and one rotational DoF is driven sinusoidally

9.4.2.1 Calculating the rotation of the rotational driver

```
AnyFolder &PlatePara =...HumanModel.Mannequin.PlateModel;
AnyFolder &PlateDim = ..Environment.Origin.Plate;
```

```
AnyVar DegreeRot =
asin((PlatePara.Amplitude)/(PlatePara.DistanceFeetApart/2
));
```

9.4.2.2 Drivers

```
AnyFolder Drivers =
{
AnyKinEqSimpleDriver PlateCOMlin =
  {
    AnyKinLinear &Linear = ..KinematicMeasures.PlateLin;
    MeasureOrganizer = {0,1,2};
    DriverPos = ..PlateDim.r0;
    DriverVel = {0,0,0};
    Reaction.Type = {On,On,On};
  };

AnyKinEqSimpleDriver PlateCOMrotfixed =
  {
    AnyKinRotational &Rotational =
..KinematicMeasures.PlateRot;
    MeasureOrganizer = {0,1};
    DriverVel = {0,0};
    Reaction.Type = {On,On};
  };

AnyKinEqFourierDriver PlateCOMrotdriven =
  {
    AnyKinRotational &Rotational =
..KinematicMeasures.PlateRot;
    MeasureOrganizer = {2};
    Type = Sin;
    Freq = ..PlatePara.Frequency;
    A = {{0.0, ..DegreeRot}};
    B = {{0.0,0.0}};
    Reaction.Type = {On};
  };
```

9.4.3 Vertical WBV

In this section two linear DoF are fixed, one linear DoF is sinusoidally driven, and three rotationally DoF are fixed.

9.4.3.1 Drivers

```
AnyKinEqSimpleDriver PlateCOMlin =
  {
    AnyKinLinear &Linear = ..KinematicMeasures.PlateLin;
    MeasureOrganizer = {0,2};
    DriverPos = {..PlateDim.r0[0],..PlateDim.r0[2]};
    DriverVel = {0,0};
    Reaction.Type = {On,On};
  };

AnyKinEqFourierDriver PlateCOMlindriver =
{
  AnyKinLinear &Linear = ..KinematicMeasures.PlateLin2;
  MeasureOrganizer = {1};
  Type = Sin;
  Freq = ..PlatePara.Frequency;
  A = {{0, ..PlatePara.Amplitude}};
  B = {{0.0, 0.0}};
  Reaction.Type = {On};
};

AnyKinEqSimpleDriver PlateCOMrotfixed =
  {
    AnyKinRotational &Rotational =
..KinematicMeasures.PlateRot;
    MeasureOrganizer = {0,1,2};
    DriverVel = {0,0,0};
    Reaction.Type = {On,On,On};
  };
```

9.4.4 Shared drivers

In this section the position of the heel and toe of each foot are fixed relative to the platform and are the same for both the simulation of vertical and side-alternating vibration.

```
AnyKinEqSimpleDriver HeelR =
{
  AnyKinLinear &Linear = ..KinematicMeasures.HeelPosR;
  MeasureOrganizer = {0,1,2};
  DriverPos = {..HeelXRel,..HeelToeYRel,..HeelZRel};
  DriverVel = {0,0,0};
  Reaction.Type = {Off,Off,Off};
};
```

```
AnyKinEqSimpleDriver HeelL =
{
  AnyKinLinear &Linear = ..KinematicMeasures.HeelPosL;
  MeasureOrganizer = {0,1,2};
  DriverPos = {..HeelXRel,..HeelToeYRel,-..HeelZRel};
  DriverVel = {0,0,0};
  Reaction.Type = {Off,Off,Off};
};

AnyKinEqSimpleDriver ToeR =
{
  AnyKinLinear &Linear = ..KinematicMeasures.ToePosR;
  MeasureOrganizer = {1,2};
  DriverPos = {..HeelToeYRel,..ToeZRel};
  DriverVel = {0,0};
  Reaction.Type = {Off,Off};
};

AnyKinEqSimpleDriver ToeL =
{
  AnyKinLinear &Linear = ..KinematicMeasures.ToePosL;
  MeasureOrganizer = {1,2};
  DriverPos = {..HeelToeYRel,-..ToeZRel};
  DriverVel = {0,0};
  Reaction.Type = {Off,Off};
};

AnyKinEqSimpleDriver PelvisDriverz =
{
  AnyKinLinear &Linear = ..KinematicMeasures.Pelvis;
  MeasureOrganizer = {2};
  DriverPos =
{Main.HumanModel.Mannequin.Posture.PelvisPosZ};
  DriverVel = {0.0};
  Reaction.Type = {Off};
};

AnyKinEqSimpleDriver LumbarDriverRot =
{
  AnyKinRotational &Rot = ..KinematicMeasures.LumbarRot;
  DriverPos =
{Main.HumanModel.Mannequin.Posture.PelvisRotZ * (pi/180),
0, 0};
  DriverVel = {0,0,0};
  Reaction.Type = {Off,Off,Off};
};
```

9.5 Reaction forces

In this section reaction forces are specified at the foot relative to the ground.

```
AnyFolder Reactions =
{
AnyReacForce RightFootReaction =
    {
      AnyKinRotational rot =
      {
        AnySeg &ref1=
Main.HumanModel.BodyModel.Right.Leg.Seg.Foot;
        AnySeg &ref2=
Main.Model.Environment.Origin.Plate;
        Type = RotVector;
        AngVelOnOff = On;
      };

      AnyKinLinear RightFootLinMeasure =
      {
        AnySeg &ref1=
Main.HumanModel.BodyModel.Right.Leg.Seg.Foot;
        AnySeg &ref2=
Main.Model.Environment.Origin.Plate;
      };
    };

    AnyReacForce LeftFootReaction =
    {
      AnyKinRotational rot =
      {
        AnySeg &ref1=
Main.HumanModel.BodyModel.Left.Leg.Seg.Foot;
        AnySeg &ref2=
Main.Model.Environment.Origin.Plate;
        Type = RotVector;
        AngVelOnOff = On;
      };

      AnyKinLinear RightFootLinMeasure =
      {
        AnySeg &ref1=
Main.HumanModel.BodyModel.Left.Leg.Seg.Foot;
        AnySeg &ref2=
Main.Model.Environment.Origin.Plate;
      };
```

```
    };
```

9.6 Reference frame

The global reference frame used during the analysis.

```
AnyFixedRefFrame GlobalRef =
{
  Origin={0, 0, 0};
  AnyDrawRefFrame DrwRef =
  {
  ScaleXYZ={0.5,0.5,0.5};
  RGB ={1,0,0}  ;
  };
};
```

9.7 Force measures

For muscles which were split into several fibres, the overall force of the muscle was calculated by the summation of these.

```
AnyFolder ForceMeasures =
{
AnyForceMomentMeasure2 RectusFemoris =
{
  AnyRefFrame &Ref = Main.Model.Environment.Origin;
  AnySeg &seg1=
Main.HumanModel.BodyModel.Right.Leg.Seg.Patella;

  AnyForceBase &mus1 =
Main.HumanModel.BodyModel.Right.Leg.Mus.RectusFemoris1;
  AnyForceBase &mus2 =
Main.HumanModel.BodyModel.Right.Leg.Mus.RectusFemoris2;

  AnyVar Magnitude = (F[0]^2 + F[1]^2 + F[2]^2)^0.5;
};

AnyForceMomentMeasure2 VastusLateralis =
{
  AnyRefFrame &Ref = Main.Model.Environment.Origin;
  AnySeg &seg1=
Main.HumanModel.BodyModel.Right.Leg.Seg.Patella;

  AnyForceBase &mus1 =
Main.HumanModel.BodyModel.Right.Leg.Mus.VastusLateralisIn
ferior1;
```

```
  AnyForceBase &mus2 =
Main.HumanModel.BodyModel.Right.Leg.Mus.VastusLateralisIn
ferior2;
  AnyForceBase &mus3 =
Main.HumanModel.BodyModel.Right.Leg.Mus.VastusLateralisIn
ferior3;
  AnyForceBase &mus4 =
Main.HumanModel.BodyModel.Right.Leg.Mus.VastusLateralisIn
ferior4;
  AnyForceBase &mus5 =
Main.HumanModel.BodyModel.Right.Leg.Mus.VastusLateralisIn
ferior5;
  AnyForceBase &mus6 =
Main.HumanModel.BodyModel.Right.Leg.Mus.VastusLateralisIn
ferior6;
  AnyForceBase &mus7 =
Main.HumanModel.BodyModel.Right.Leg.Mus.VastusLateralisSu
perior1;
  AnyForceBase &mus8 =
Main.HumanModel.BodyModel.Right.Leg.Mus.VastusLateralisSu
perior2;

  AnyVar Magnitude = (F[0]^2 + F[1]^2 + F[2]^2)^0.5;
};

AnyForceMomentMeasure2 BicepsFemoris =
{
  AnyRefFrame &Ref = Main.Model.Environment.Origin;
  AnySeg &seg1=
Main.HumanModel.BodyModel.Right.Leg.Seg.PelvisSeg;
  AnySeg &seg2=
Main.HumanModel.BodyModel.Right.Leg.Seg.Thigh;

  AnyForceBase &mus1 =
Main.HumanModel.BodyModel.Right.Leg.Mus.BicepsFemorisCapu
tLongum1;
  AnyForceBase &mus2 =
Main.HumanModel.BodyModel.Right.Leg.Mus.BicepsFemorisCapu
tBreve1;
  AnyForceBase &mus3 =
Main.HumanModel.BodyModel.Right.Leg.Mus.BicepsFemorisCapu
tBreve2;
  AnyForceBase &mus4 =
Main.HumanModel.BodyModel.Right.Leg.Mus.BicepsFemorisCapu
tBreve3;
  AnyVar Magnitude = (F[0]^2 + F[1]^2 + F[2]^2)^0.5;
```

```
};

AnyForceMomentMeasure2 GluteusMaximus =
{
  AnyRefFrame &Ref = Main.Model.Environment.Origin;
  AnySeg &seg1=
Main.HumanModel.BodyModel.Right.Leg.Seg.PelvisSeg;

  AnyForceBase &mus1 =
Main.HumanModel.BodyModel.Right.Leg.Mus.GluteusMaximusSup
erior1;
  AnyForceBase &mus2 =
Main.HumanModel.BodyModel.Right.Leg.Mus.GluteusMaximusSup
erior2;
  AnyForceBase &mus3 =
Main.HumanModel.BodyModel.Right.Leg.Mus.GluteusMaximusSup
erior3;
  AnyForceBase &mus4 =
Main.HumanModel.BodyModel.Right.Leg.Mus.GluteusMaximusSup
erior4;
  AnyForceBase &mus5 =
Main.HumanModel.BodyModel.Right.Leg.Mus.GluteusMaximusSup
erior5;
  AnyForceBase &mus6 =
Main.HumanModel.BodyModel.Right.Leg.Mus.GluteusMaximusSup
erior6;
  AnyForceBase &mus7 =
Main.HumanModel.BodyModel.Right.Leg.Mus.GluteusMaximusInf
erior1;
  AnyForceBase &mus8 =
Main.HumanModel.BodyModel.Right.Leg.Mus.GluteusMaximusInf
erior2;
  AnyForceBase &mus9 =
Main.HumanModel.BodyModel.Right.Leg.Mus.GluteusMaximusInf
erior3;
  AnyForceBase &mus10 =
Main.HumanModel.BodyModel.Right.Leg.Mus.GluteusMaximusInf
erior4;
  AnyForceBase &mus11 =
Main.HumanModel.BodyModel.Right.Leg.Mus.GluteusMaximusInf
erior5;
  AnyForceBase &mus12 =
Main.HumanModel.BodyModel.Right.Leg.Mus.GluteusMaximusInf
erior6;
  AnyVar Magnitude = (F[0]^2 + F[1]^2 + F[2]^2)^0.5;
};
```

```
AnyForceMomentMeasure2 Gastrocnemius =
{
  AnyRefFrame &Ref = Main.Model.Environment.Origin;
  AnySeg &seg1=
Main.HumanModel.BodyModel.Right.Leg.Seg.Thigh;

  AnyForceBase &mus1 =
Main.HumanModel.BodyModel.Right.Leg.Mus.GastrocnemiusLate
ralis1;
  AnyForceBase &mus2 =
Main.HumanModel.BodyModel.Right.Leg.Mus.GastrocnemiusMedi
alis1;
  AnyVar Magnitude = (F[0]^2 + F[1]^2 + F[2]^2)^0.5;
};
};
```

9.8 Muscle activity measures

For muscles which were split into several fibres, the overall muscle activity was calculated by the mean of these values. An exception to this is the case of the envelope of the lower limbs which calculates the max muscle activity of the lower limbs.

```
AnyFolder Muscles =
    {
      AnySearchFun MuscleList =
      {
        #if ((RIGHT_LEG_TD_SIMPLE_MUSCLES) +
(RIGHT_LEG_TD_MUS_3E)) == 0
          Search =
".....Right.Leg.JointMuscles.*.*.dof0.Muscle.*.Activity";
        #else
          Search = ".....Right.Leg.Mus.*.Activity";
        #endif
      };
      AnyVar Envelope = max(MuscleList());
    }; //End Muscles

    AnyFolder RectusFemoris =
    {
      AnySearchFun MuscleList =
      {
        Search =
".....Right.Leg.Mus.RectusFemoris*.Activity";
```

```
      };
      AnyVar Envelope = mean(MuscleList());
    };

    AnyFolder VastusLateralis =
    {
      AnySearchFun MuscleList =
      {
        Search =
".....Right.Leg.Mus.VastusLateralis*.Activity";
      };
      AnyVar Envelope = mean(MuscleList());
    };

    AnyFolder BicepsFemoris =
    {
      AnySearchFun MuscleList =
      {
        Search =
".....Right.Leg.Mus.BicepsFemoris*.Activity";
      };
      AnyVar Envelope = mean(MuscleList());
    };

    AnyFolder GluteusMaximus =
    {
      AnySearchFun MuscleList =
      {
        Search =
".....Right.Leg.Mus.GluteusMaximus*.Activity";
      };
      AnyVar Envelope = mean(MuscleList());
    };

    AnyFolder Gastrocnemius =
    {
      AnySearchFun MuscleList =
      {
        Search =
".....Right.Leg.Mus.Gastrocnemius*.Activity";
      };
      AnyVar Envelope = mean(MuscleList());
    };

  }; //End Leg
```

9.9 Fat percent

The fat percentage specified to reduce the muscle mass percentage of the body model with SCI simulated by 15%.

```
AnyVar FatPercent = 25.983;
```